

Fast Imaging of Coherent and Transient MHD in DIII-D

J.H. Yu¹,

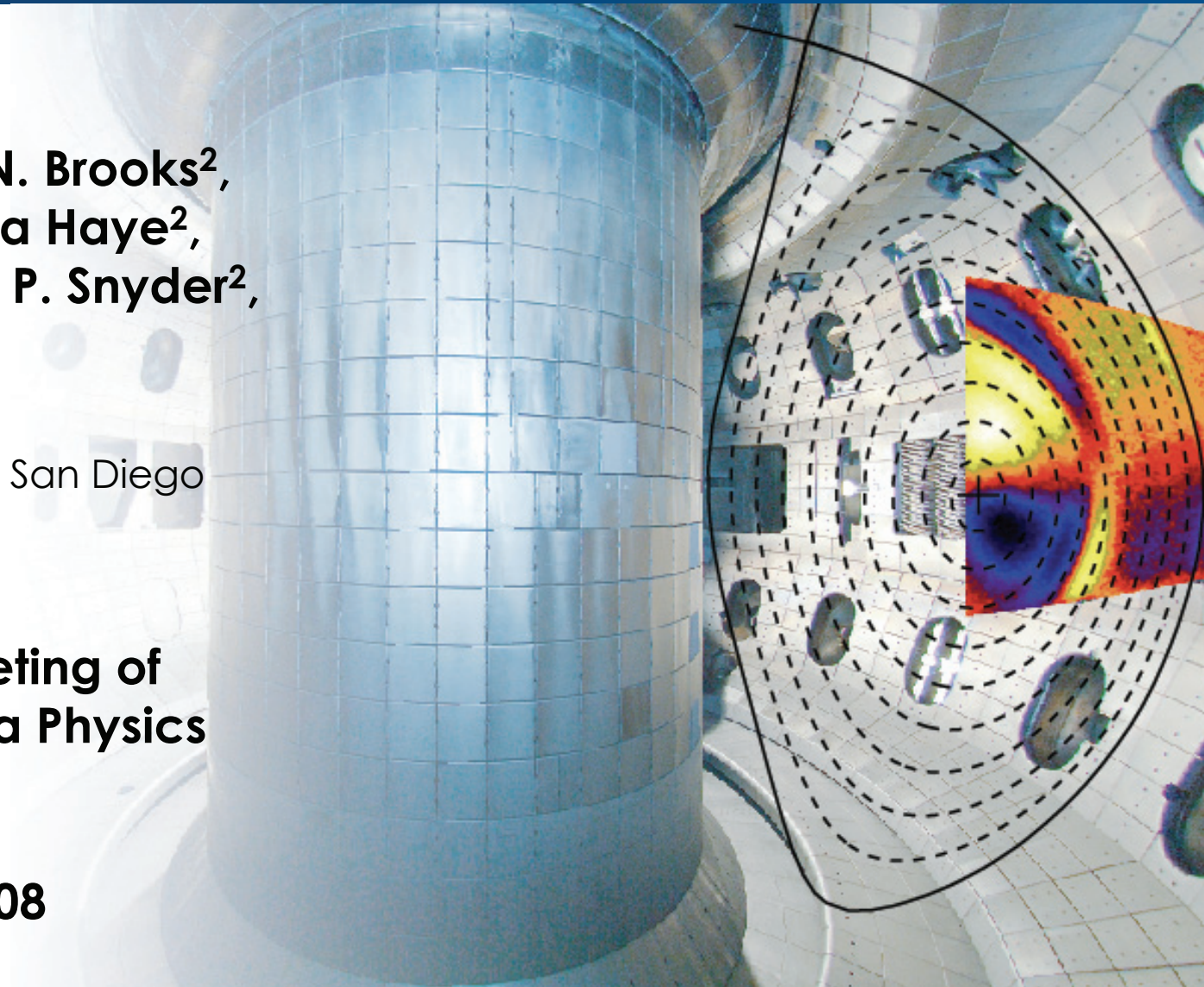
**M.A. Van Zeeland², N. Brooks²,
M. Chu², V. Izzo¹, R. La Haye²,
E. Lazarus², C. Petty², P. Snyder²,
E. Strait², A. Turnbull²
and the DIII-D team**

¹ University of California at San Diego

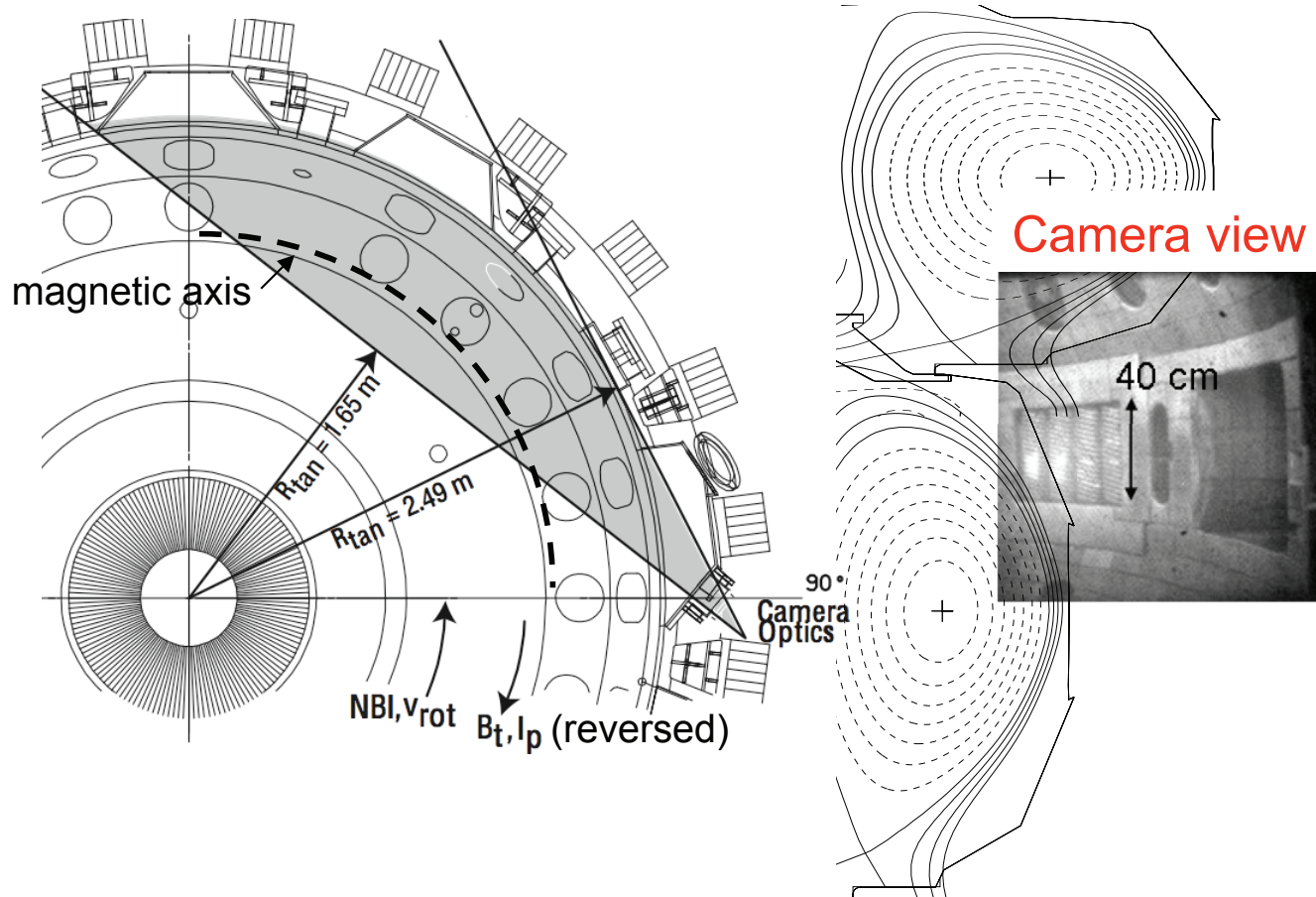
² General Atomics

**Presented at the
50th APS Annual Meeting of
the Division of Plasma Physics
Dallas, Texas**

November 17–21, 2008



The UCSD fast framing camera images a significant fraction of the plasma cross-section

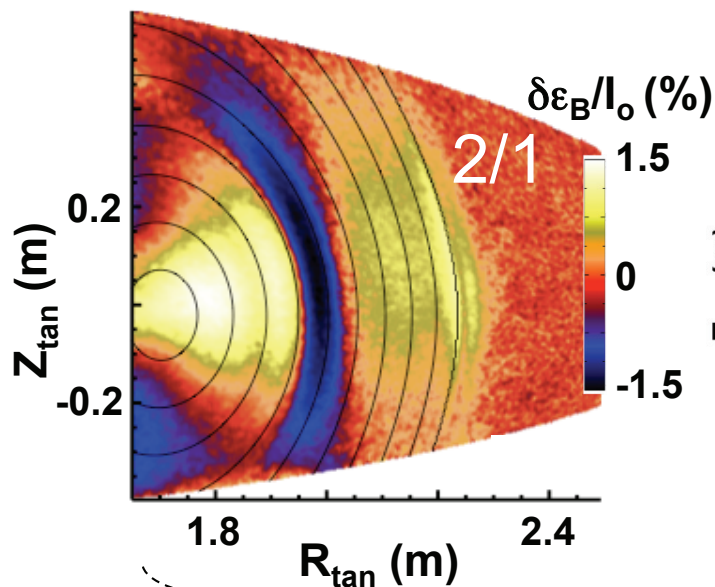


- 12 bits, up to 26 kFrames/s at 256x256 pixels, 0.2 to 0.4 cm per pixel at point of tangency.
- Camera system detects visible to near IR light ~450-950 nm.

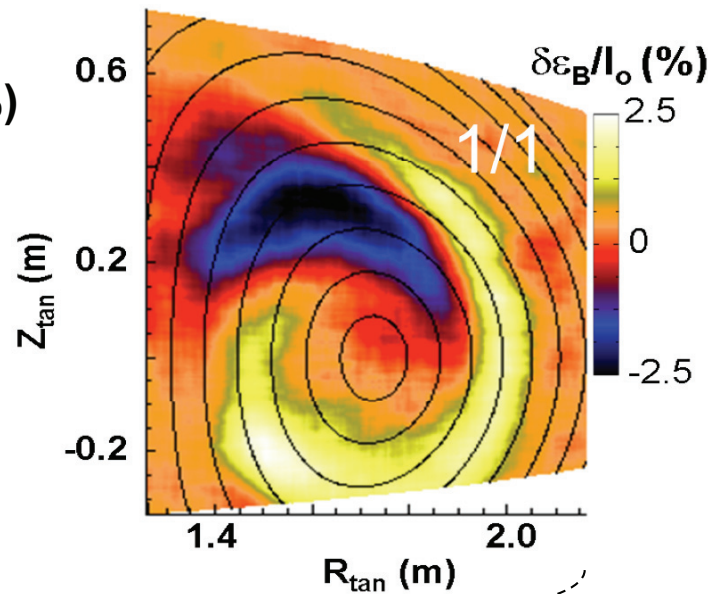
Outline

- Fast camera is used to image core MHD with unprecedented resolution.
- Imaging allows detailed comparison to stability models.

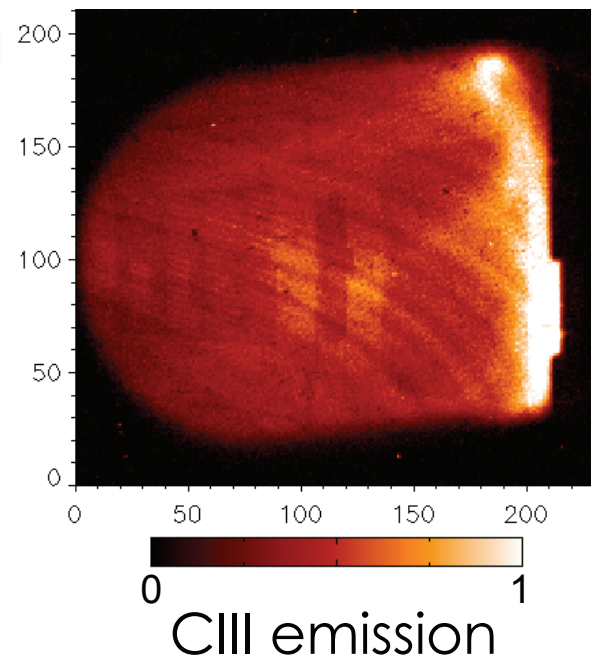
Tearing modes



Sawtooth instability

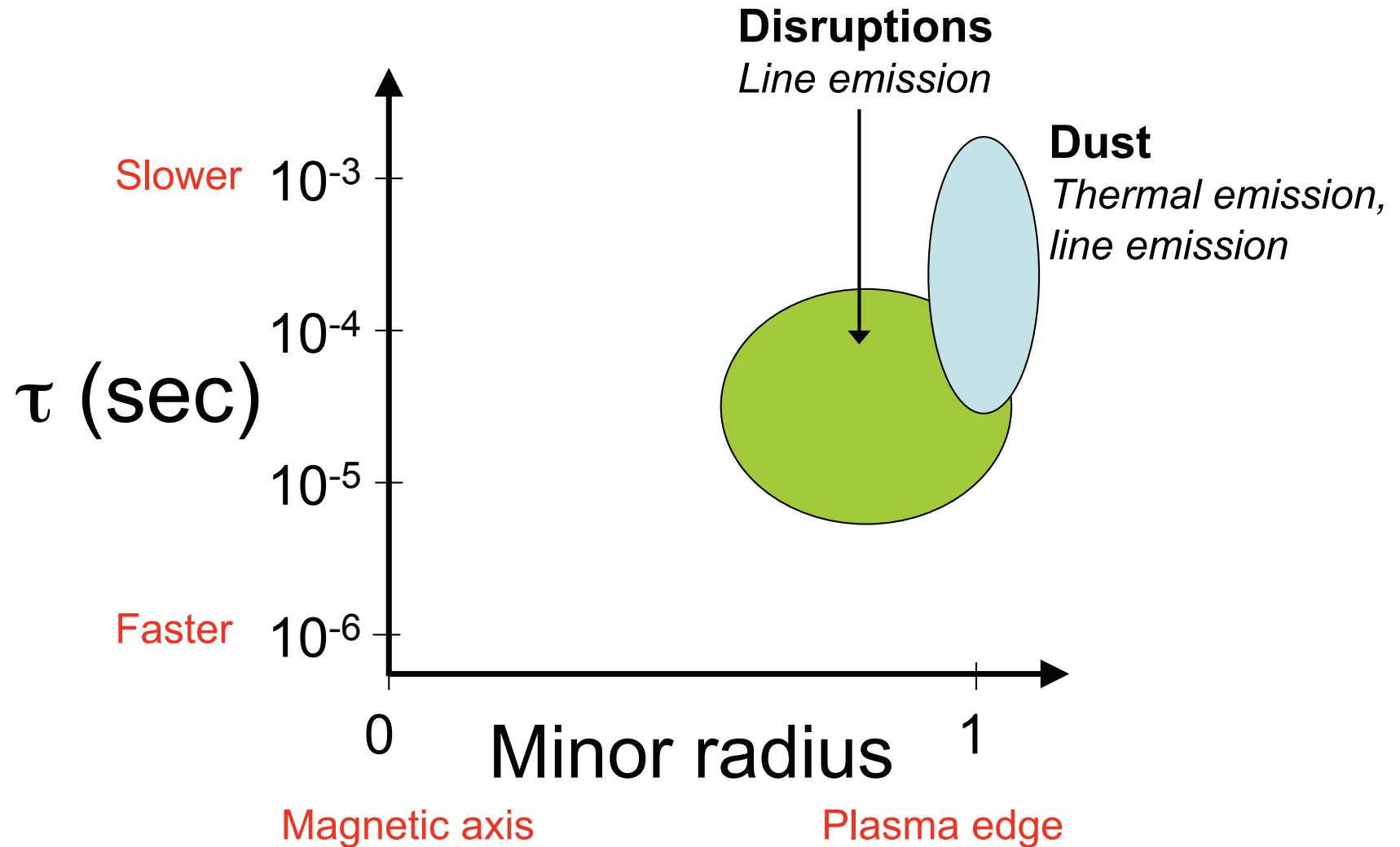


Edge localized modes (ELMs)

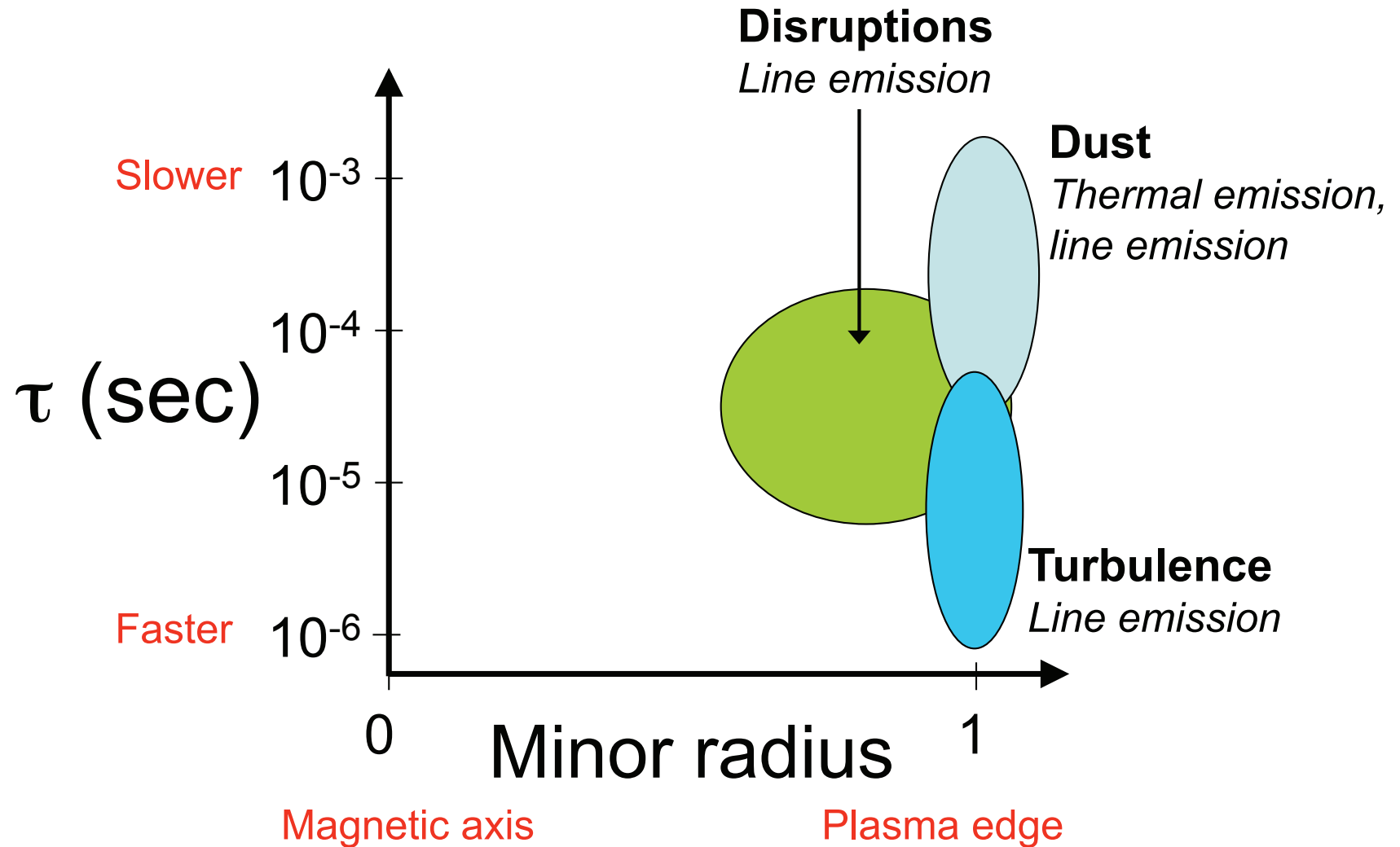


Bremsstrahlung emission

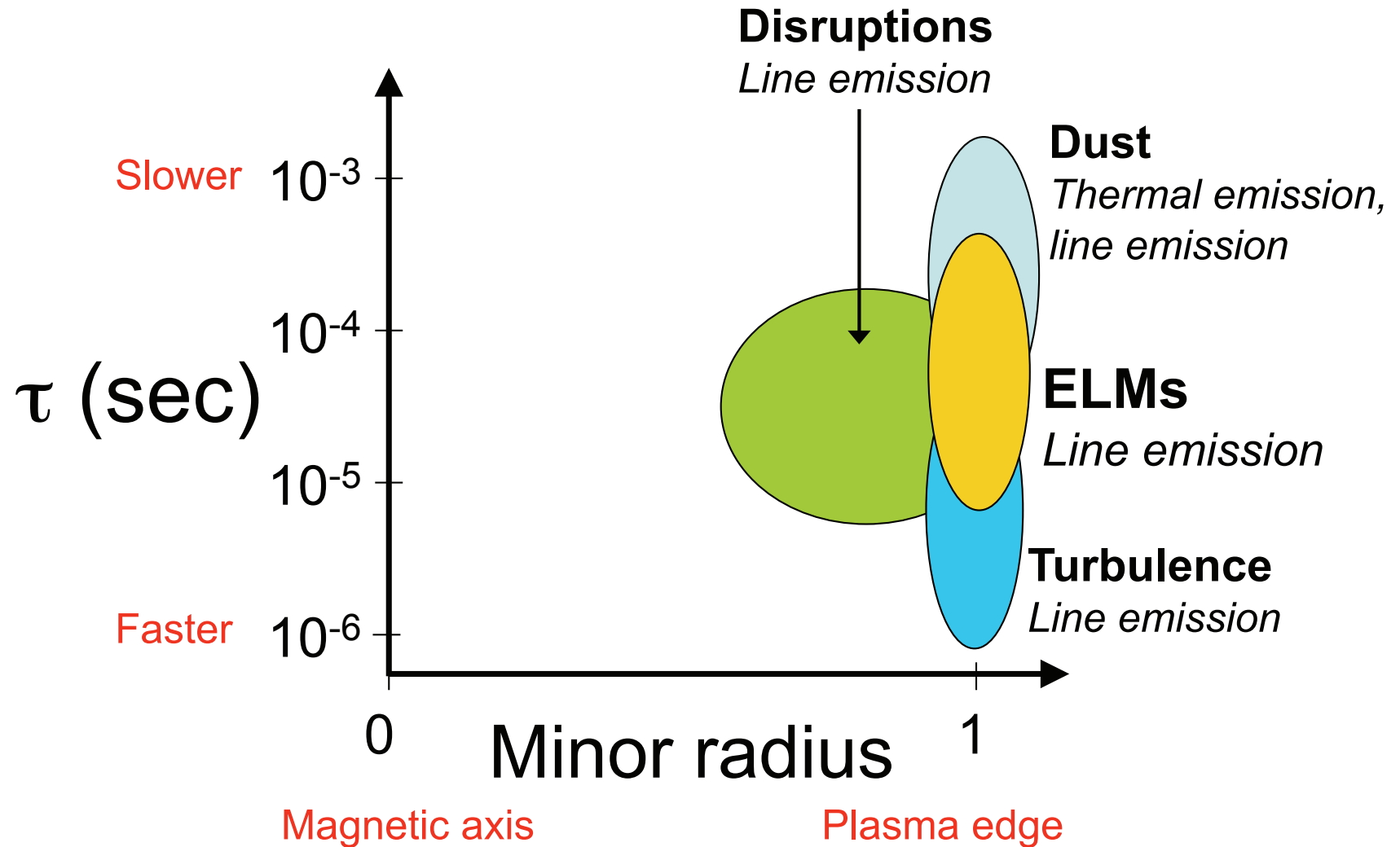
Core MHD is a new parameter space for fast visible imaging



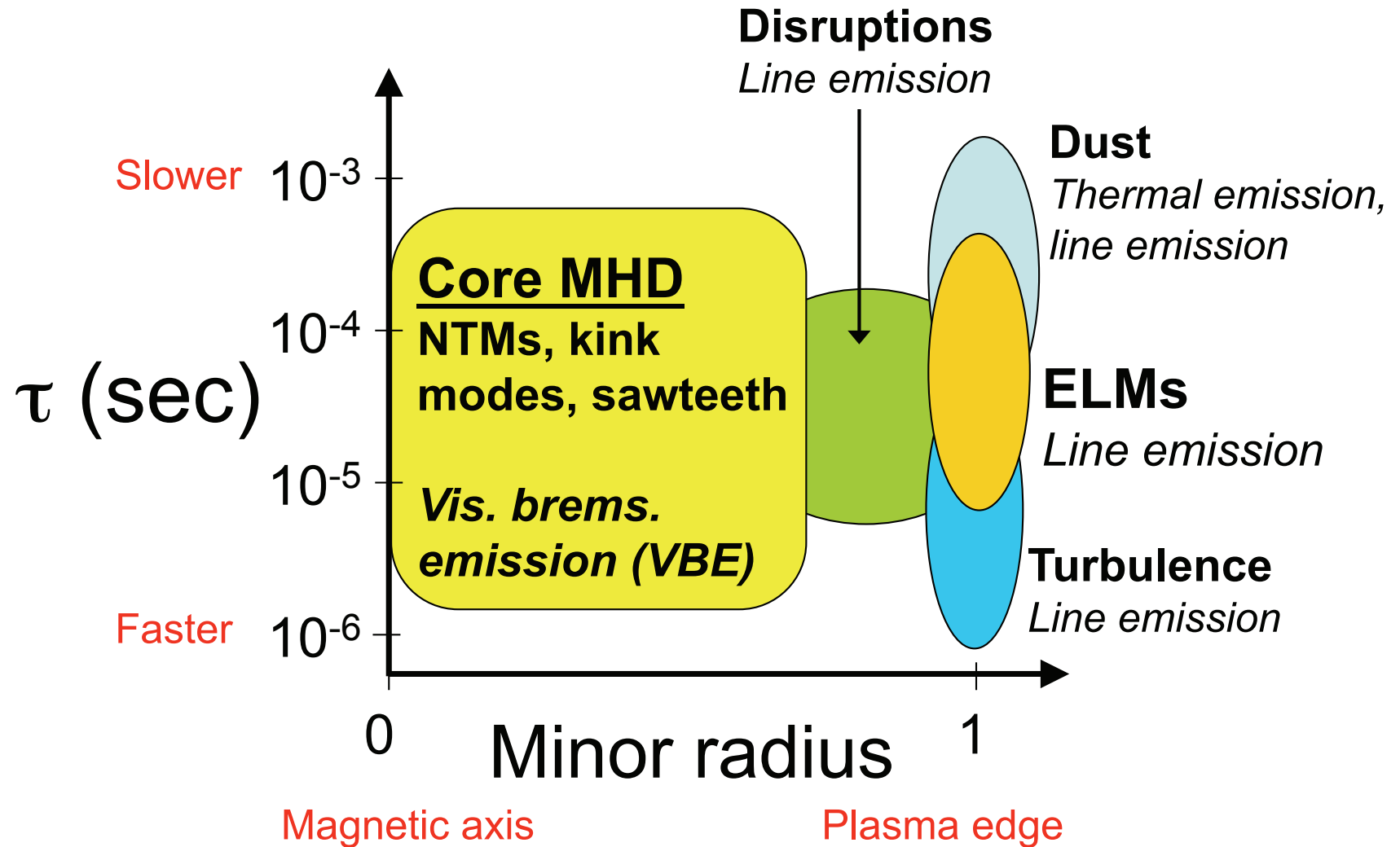
Core MHD is a new parameter space for fast visible imaging



Core MHD is a new parameter space for fast visible imaging

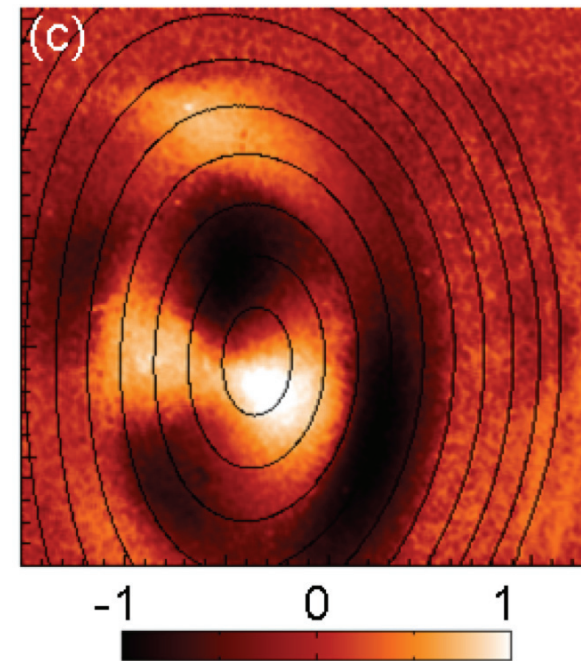


Core MHD is a new parameter space for fast visible imaging



Outline

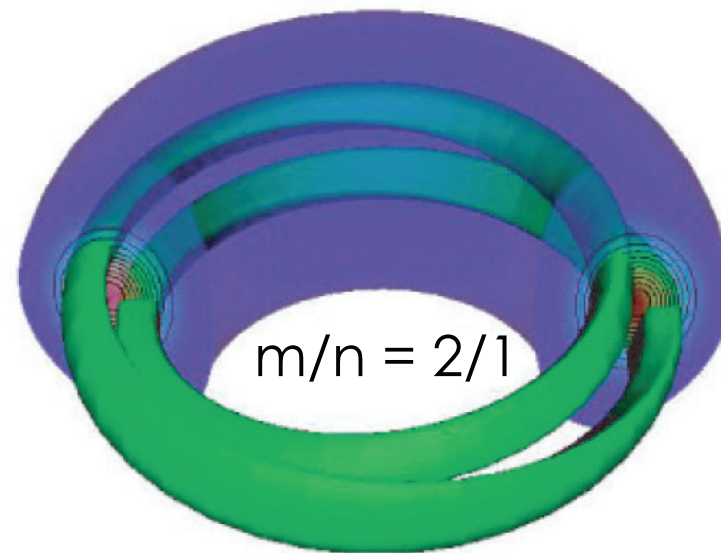
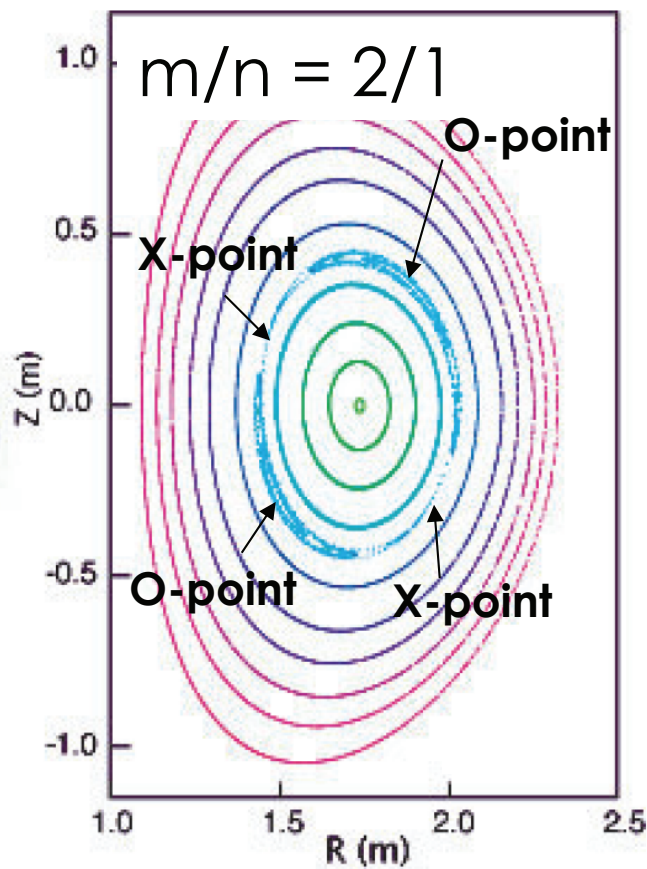
- Tearing modes.
- Sawtooth instability.
- Edge localized modes (ELMs).



Tearing modes are magnetic islands which deform magnetic surfaces

- Equilibrium flux surfaces are toroidally axisymmetric.
- Finite plasma resistivity \rightarrow toroidally non-axisymmetric helical currents break or tear magnetic field lines at **rational surfaces** $q = m/n$.

Safety factor $q = d\phi/d\theta$ gives path of magnetic field lines as they go around the torus

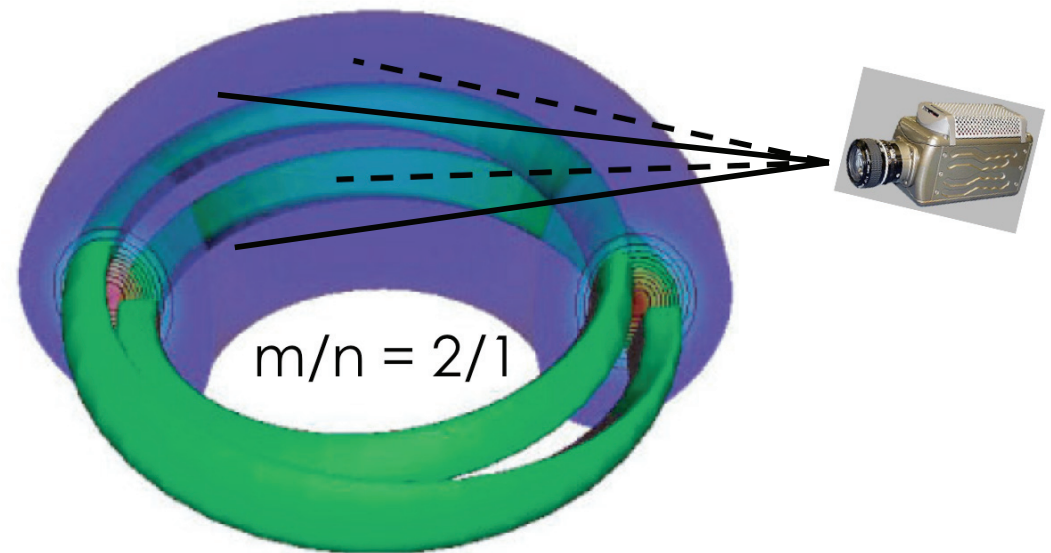
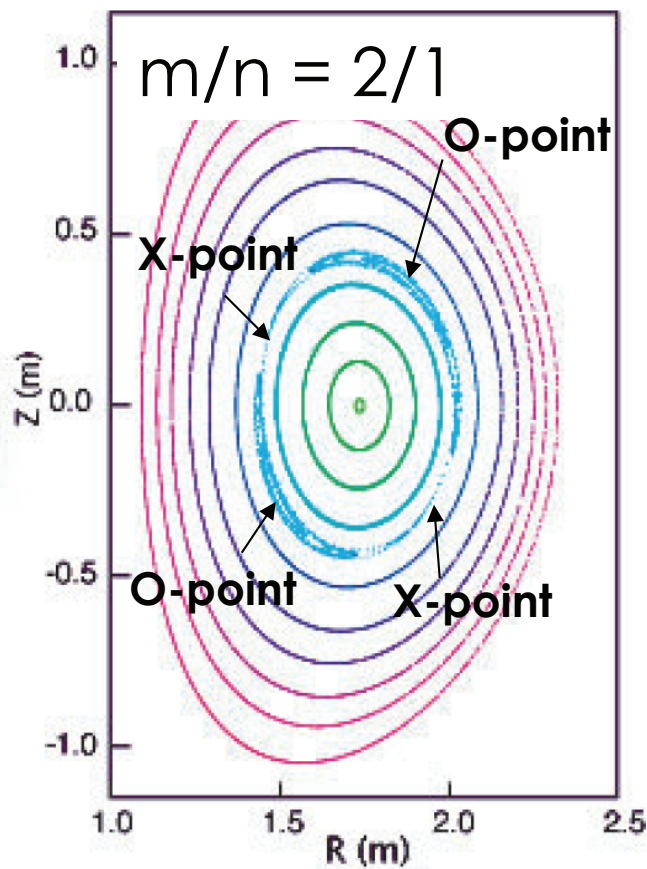


D.P. Brennan et al., 2004

Tearing modes are magnetic islands which deform magnetic surfaces

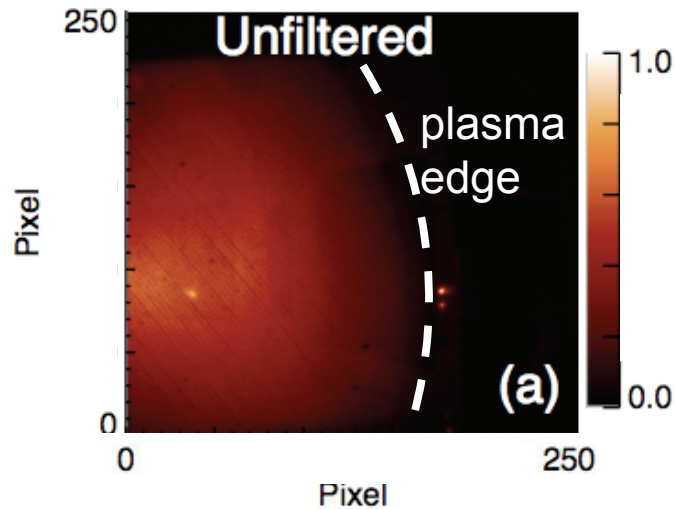
- Equilibrium flux surfaces are toroidally axisymmetric.
- Finite plasma resistivity \rightarrow toroidally non-axisymmetric helical currents break or tear magnetic field lines at **rational surfaces** $q = m/n$.

With finite toroidal rotation $d\phi/dt$, islands rotate poloidally, $d\theta/dt = 1/q d\phi/dt$.



D.P. Brennan et al., 2004

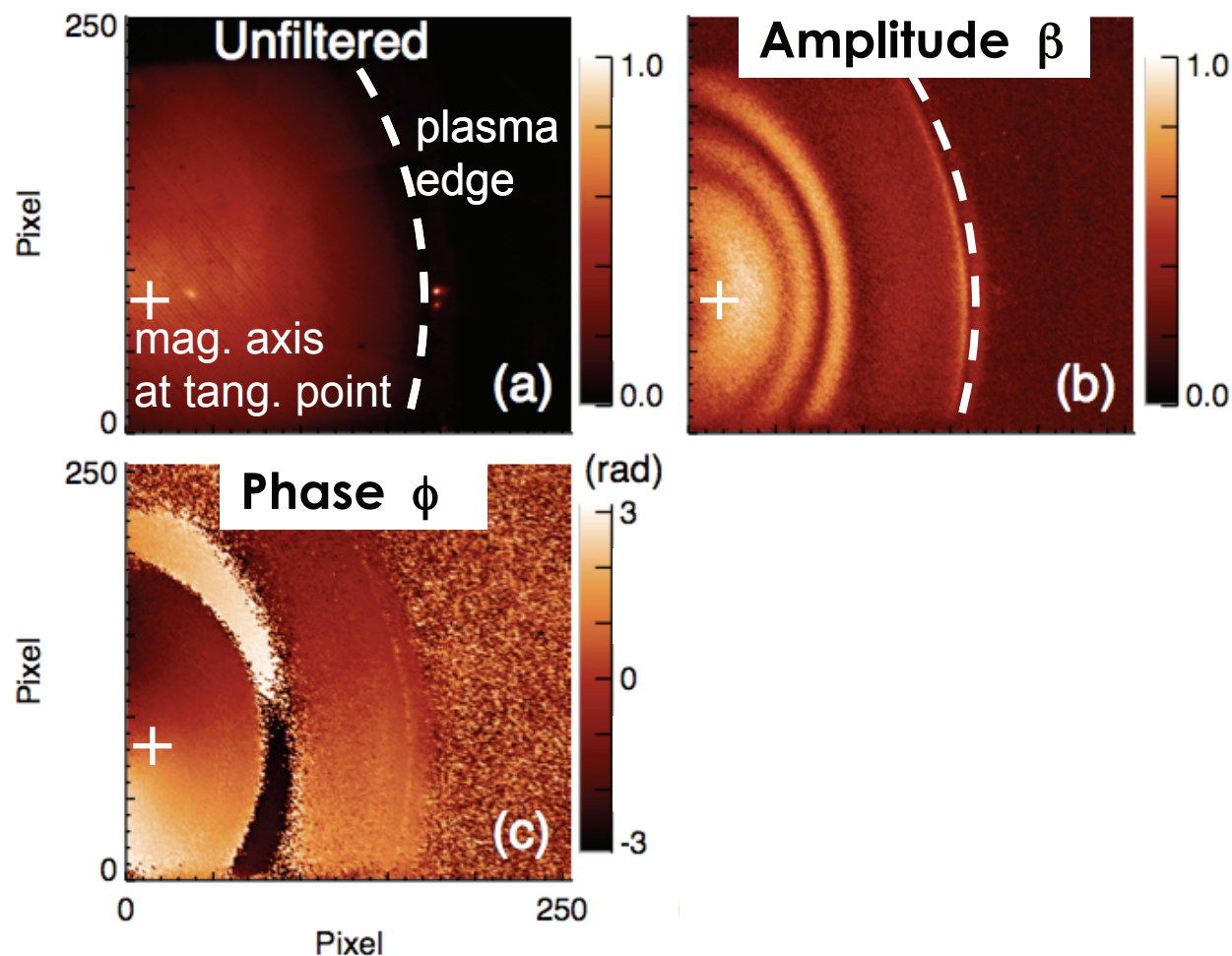
TM structure is visualized through Fourier analysis of every pixel's time series



Mode structure not visible in raw image.

Relatively high density,
 $n_e = 7 \times 10^{13} \text{ cm}^{-3}$.

TM structure is visualized through Fourier analysis of every pixel's time series



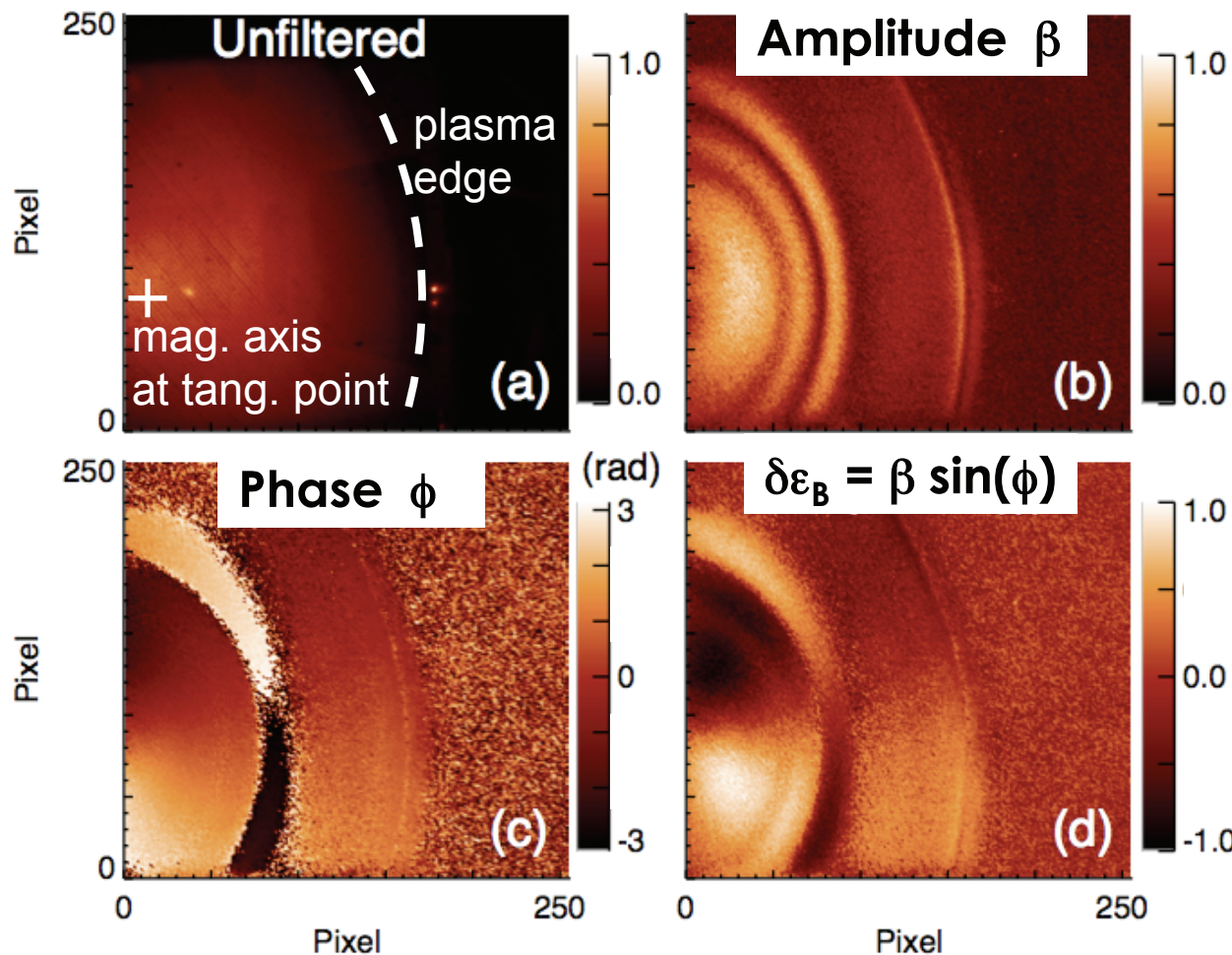
Fourier filtering at the mode frequency ($f_{\text{mode}} = 10.5 \text{ kHz}$) shows 2D amplitude and phase of mode.

256 frames used in FFT, $\Delta t_{\text{FFT}} = 10 \text{ ms}$, or ~ 100 mode periods.

Fast frame rate:
 $f_{\text{mode}} < f_{\text{Nyquist}}$

12 bit dynamic range: good S/N.

TM structure is visualized through Fourier analysis of every pixel's time series



Fourier filtering at the mode frequency ($f_{\text{mode}} = 10.5 \text{ kHz}$) shows 2D amplitude and phase of mode.

256 frames used in FFT, $\Delta t_{\text{FFT}} = 10 \text{ ms}$, or ~ 100 mode periods.

$m=2$ ($n=1$) structure seen in mode "snapshot".

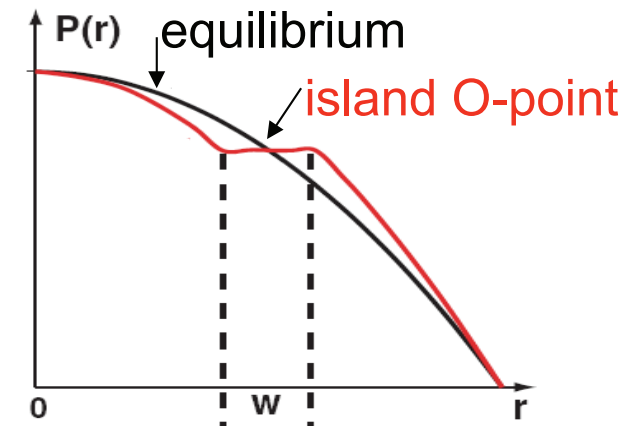
Fluctuation level in data $\frac{\delta\epsilon_B}{I_o} \approx 1\%$
total signal at mag. axis $\rightarrow I_o$

M.A. Van Zeeland, J.H. Yu, M.S. Chu, et al., Nucl. Fusion (2008).

J.H. Yu and M.A. Van Zeeland, RSI (2008).

What are we looking at?

- Island flattens pressure through the O-point.
- Null point at island center. Perturbation changes sign across island.
- Images show VBE perturbation caused by rotating islands.
- VBE is mainly sensitive to changes in density.



Visible bremsstrahlung emission (VBE)

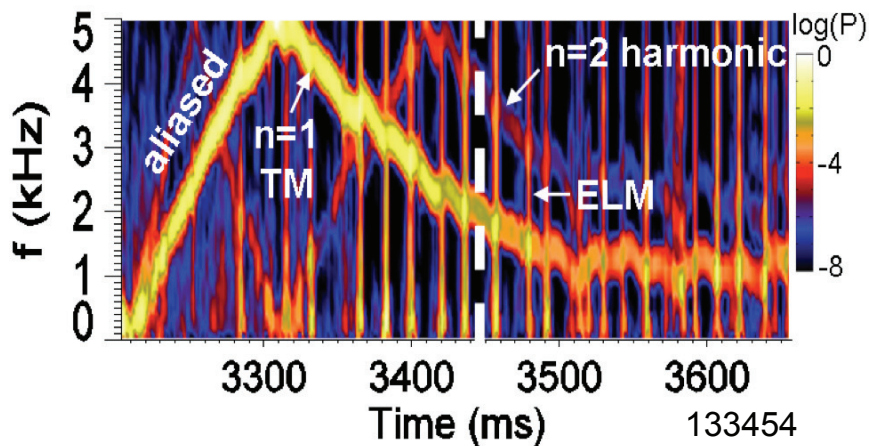
$$\frac{d\varepsilon_B}{d\lambda} = 2.85 \times 10^{-13} \frac{n_e^2 Z_{eff}}{\lambda T_e^{1/2}} e^{-\hbar c / \lambda T_e}$$

Perturbed VBE $\tilde{\varepsilon}_B \approx \zeta \cdot \nabla \varepsilon_B$

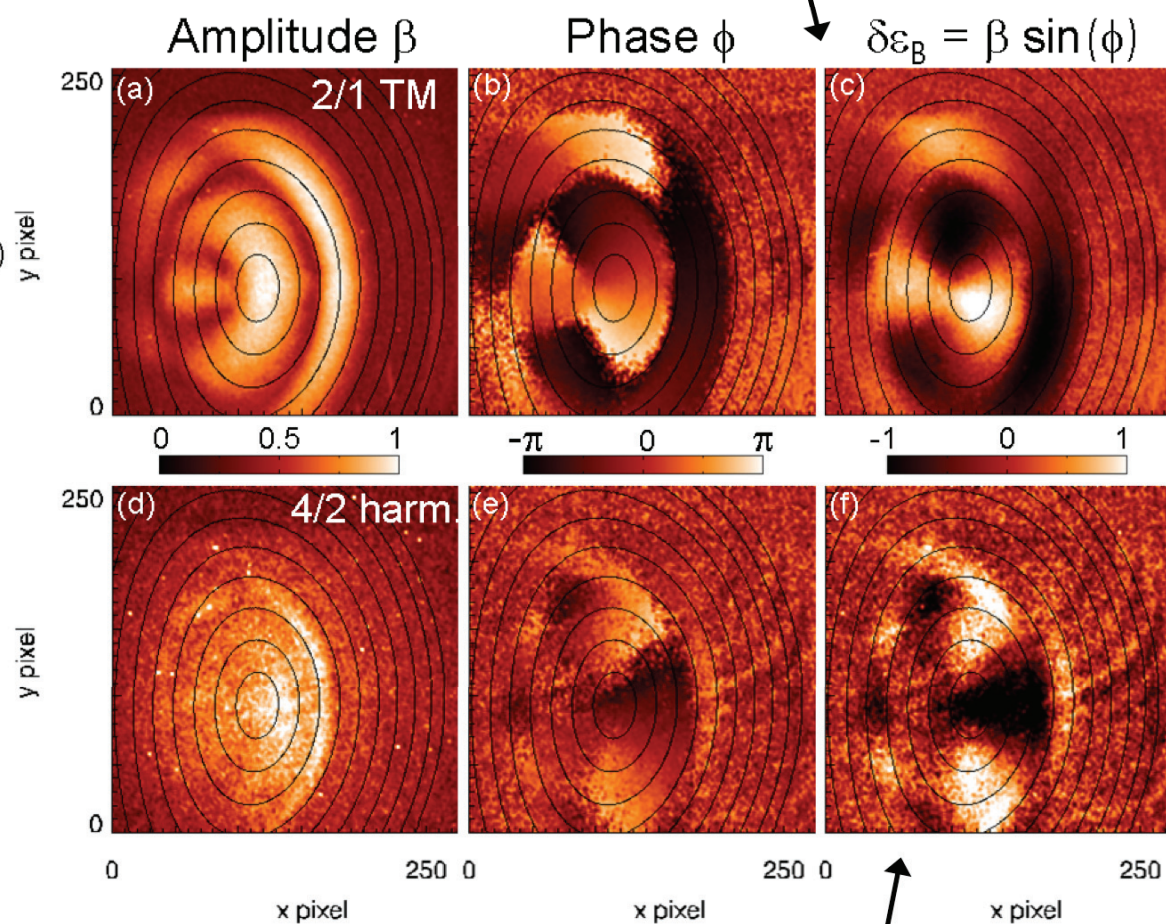
↑
field line displacement

Fundamental and harm. structures are obtained from same data using different filter frequencies

Crosspower between camera intensity and Mirnov magnetic probe



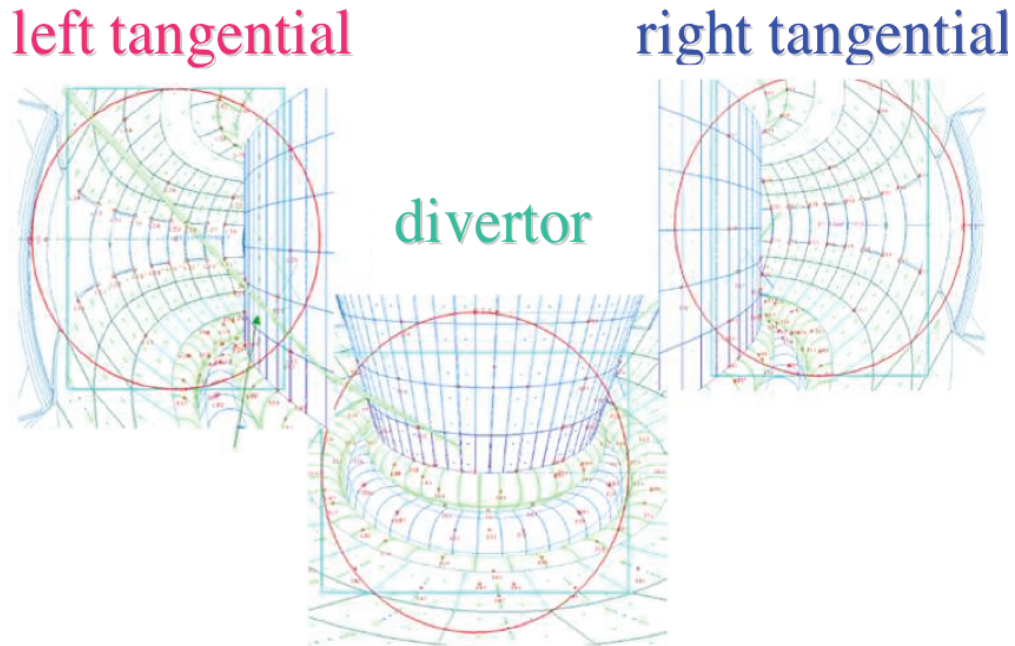
$$f = 2 \text{ kHz}, m/n = 2/1$$



$$f = 4 \text{ kHz}, 4/2 \text{ harmonic}$$

What does this mean for ITER and future devices?

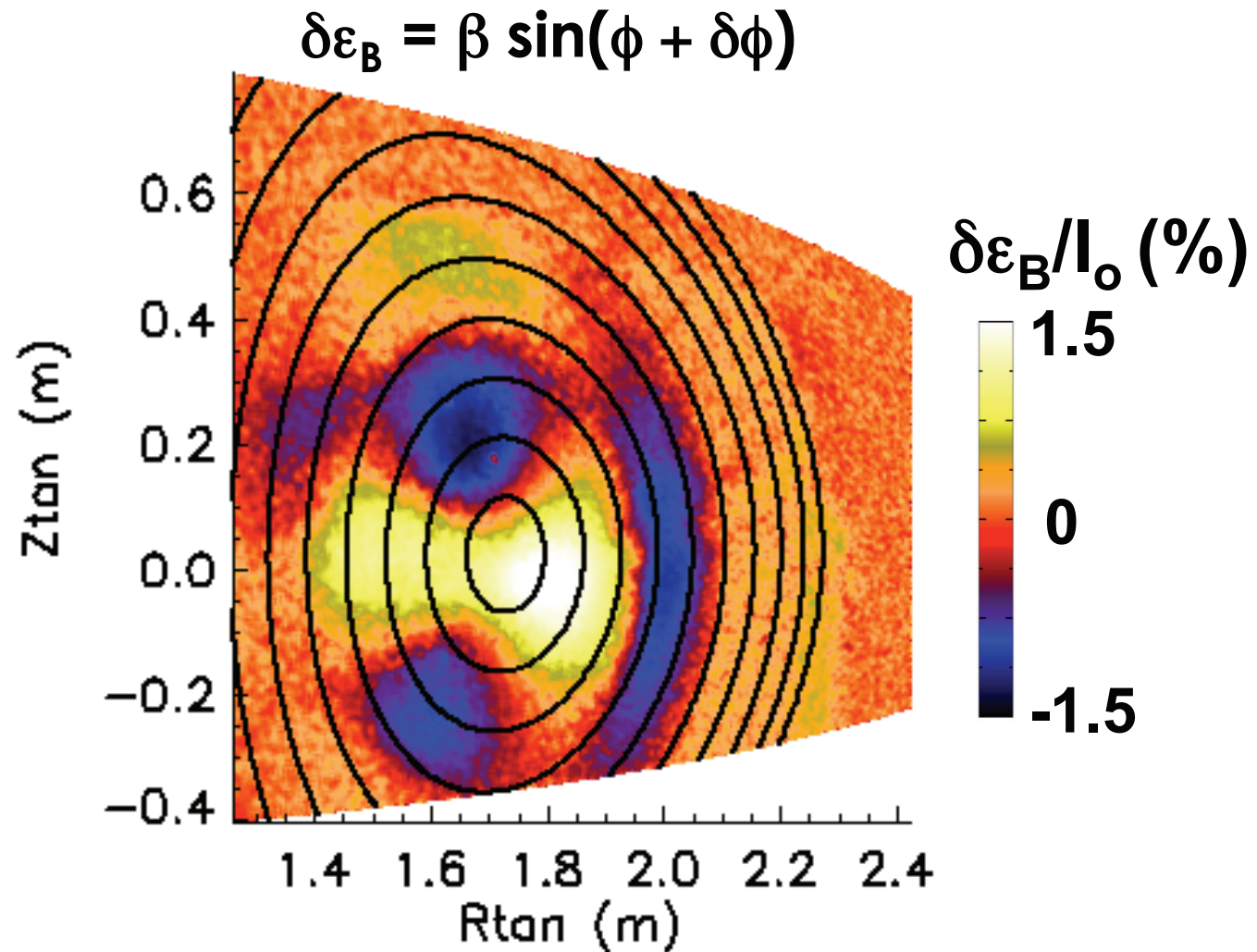
Imaging Views on ITER



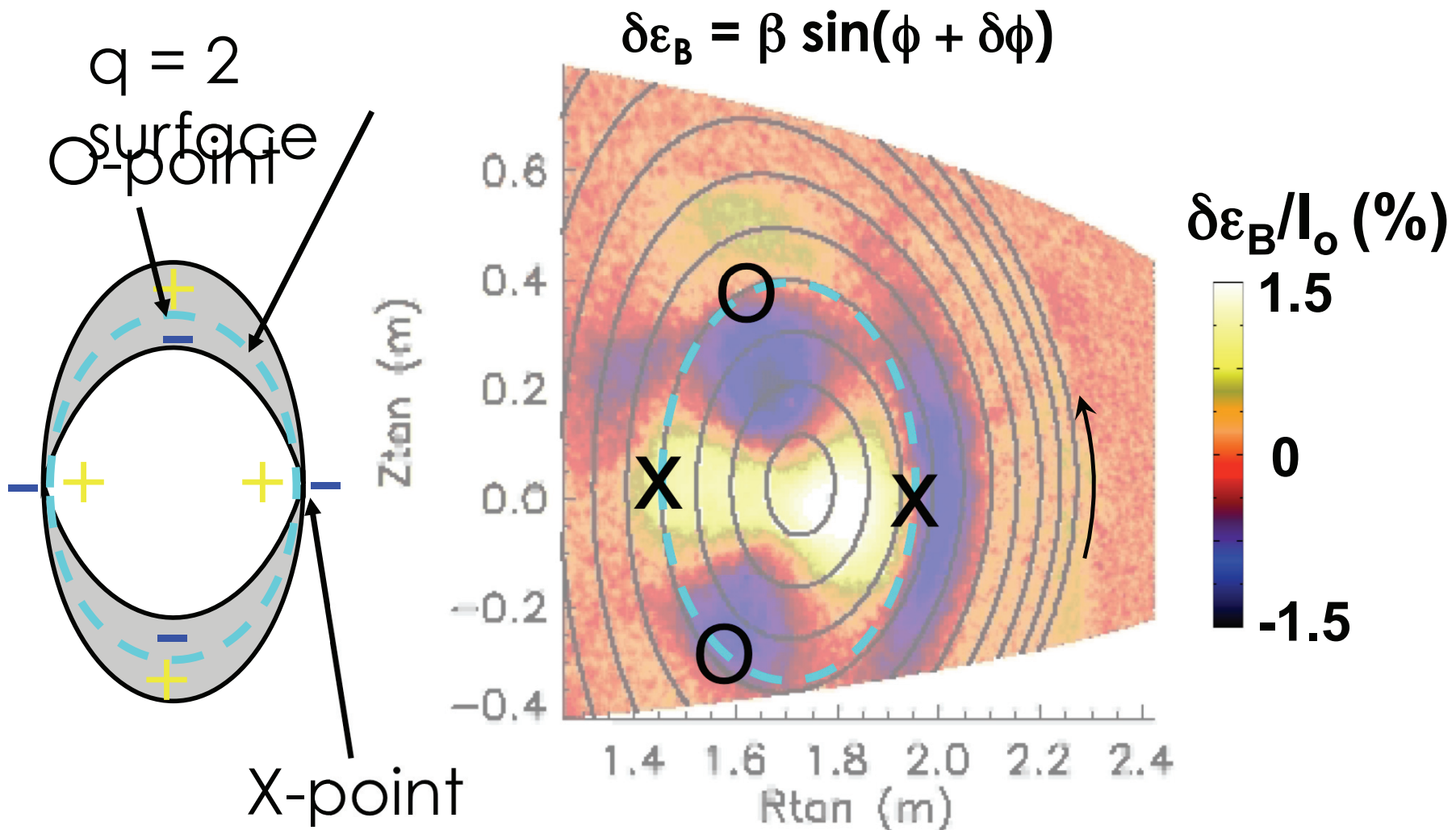
M. Davi, et.al., "Progress of the ITER Equatorial VIS/IR Wide Angle Viewing System optical design", *HTPD, Albuquerque NM (2008)*

- ITER will have tangential imaging views.
- Reasons why this technique will work better in ITER:
 - Longer path length.
 - Higher density.
 - Better cameras available -14 bit (or more) vs. 12 bit.
 - Intensifiers also available.
 - Low rotation frequencies mean longer exposure and more signal.

Time series of images shows poloidal mode rotation. Here, phase is advanced.

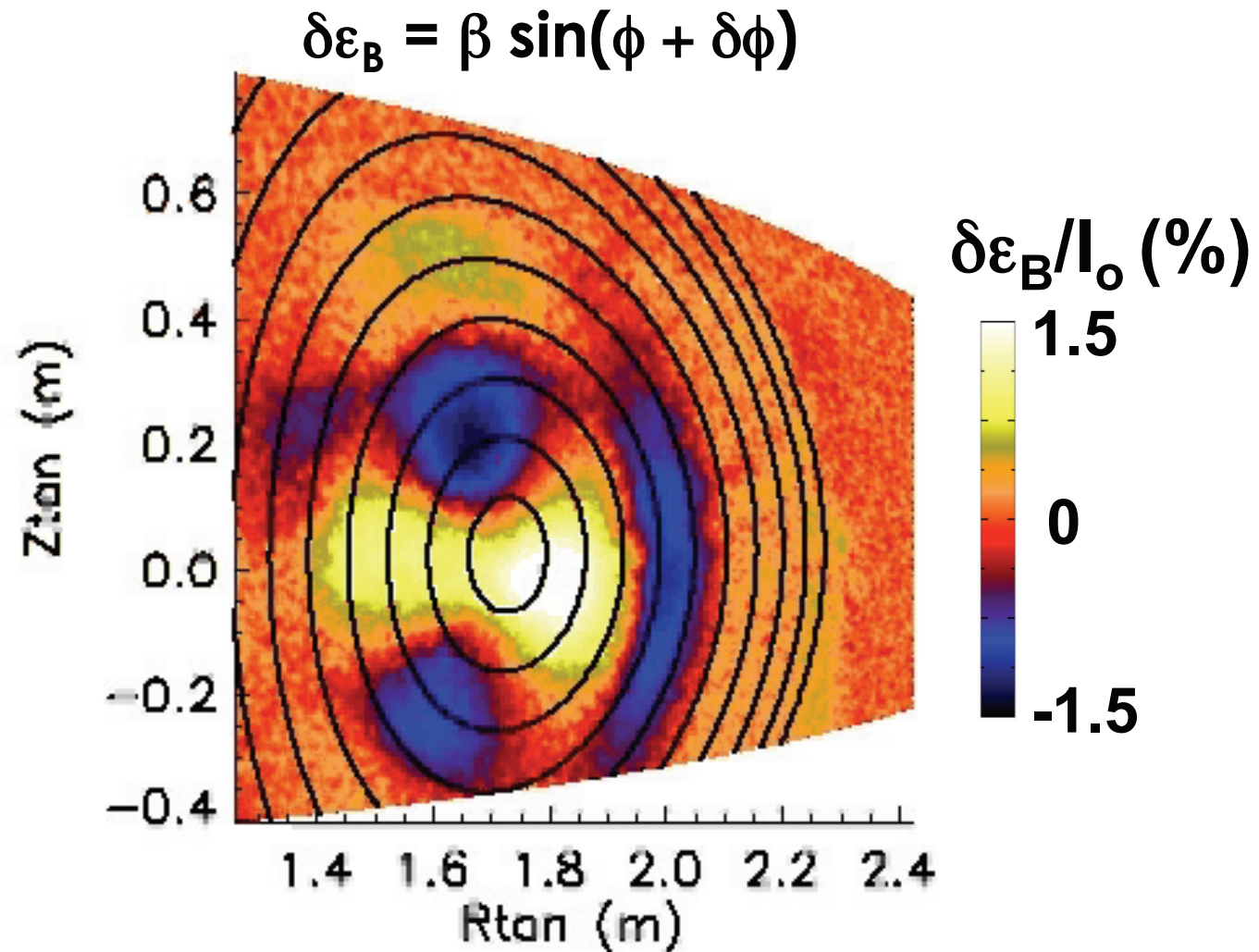


Time series of images shows poloidal mode rotation. Here, phase is advanced.

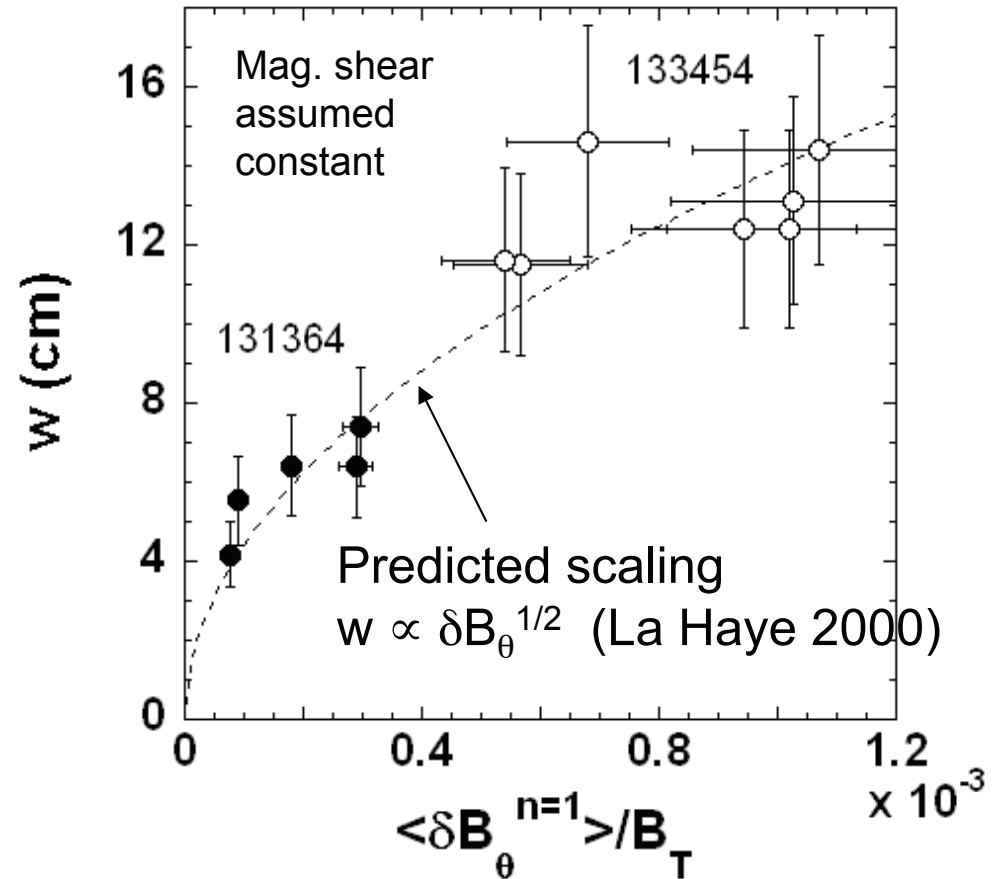
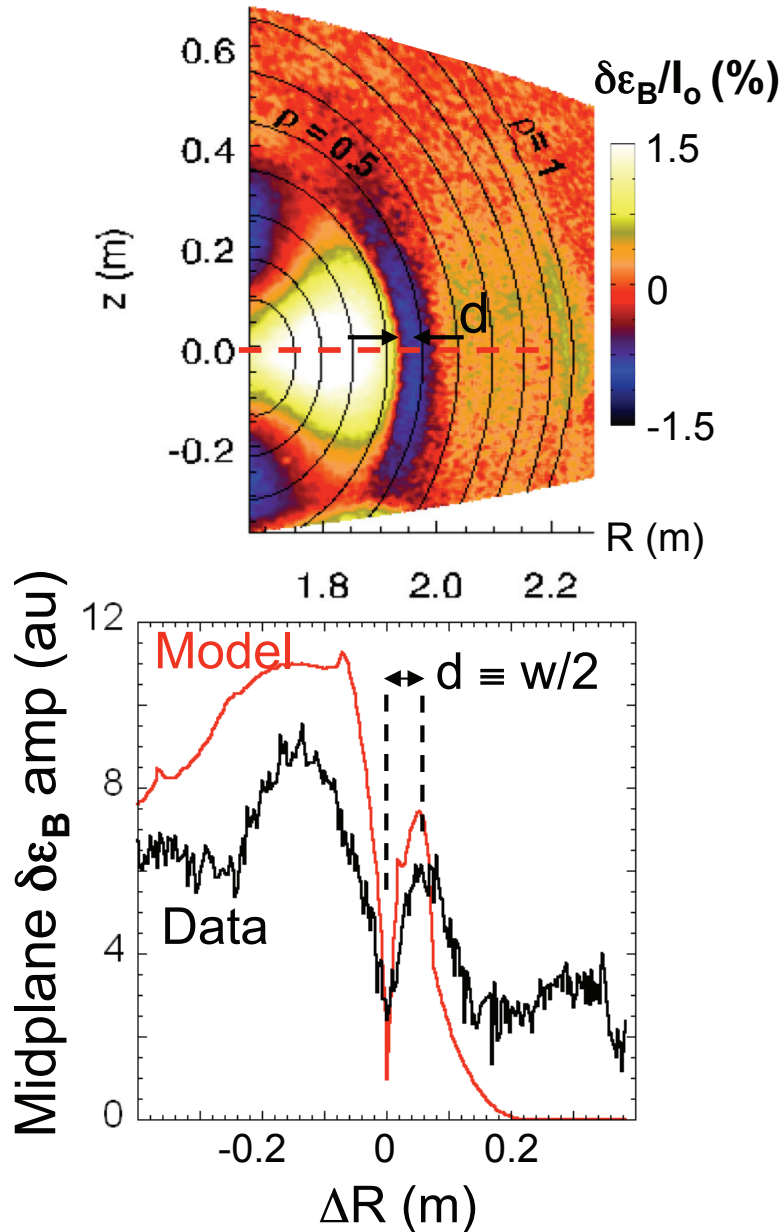


m=2 island

Time series of images shows poloidal mode rotation. Here, phase is advanced.



Imaging may be used to measure island location and width



Using future fast cameras with real time output, imaging could potentially be used to steer ECCD for NTM control in ITER.

Synthetic camera diagnostic is applied to analytic model of 2/1 island structure

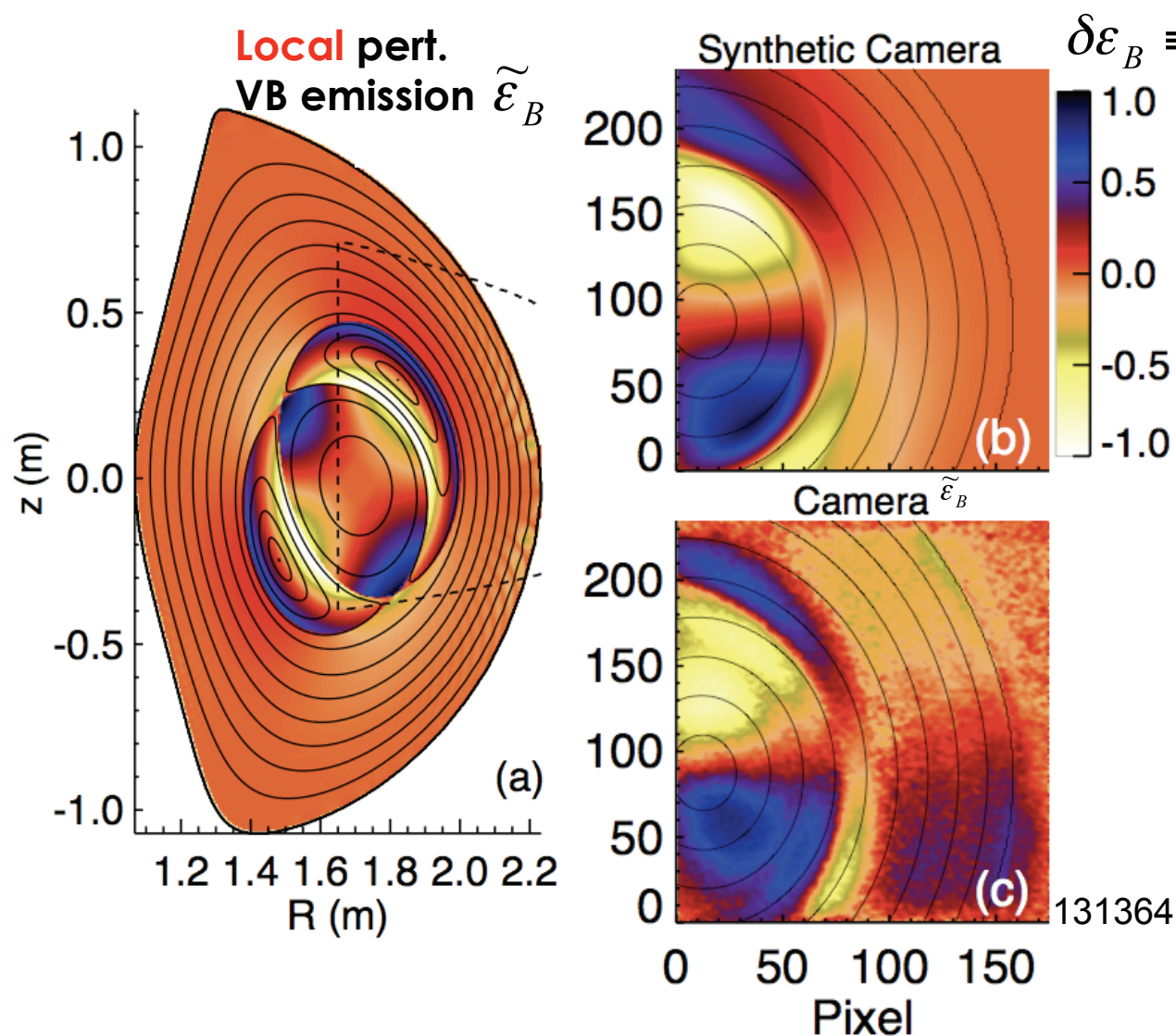
- **Model of perturbed helical flux¹** ($F = F_o + \tilde{F}$) gives perturbed VB emission:

$$F = F_o + \tilde{F}$$

- **Synthetic camera diagnostic:**
 - **Line integration** of 3D $\tilde{\mathcal{E}}_B$
 - **Finite exposure time** simulated.
 - Allows direct comparison with experiment.
 - Useful because inverting non-axisymmetric data is nontrivial.

¹ E. Strumberger, et.al., *New J. Phys*, **10**, 023017 (2008)

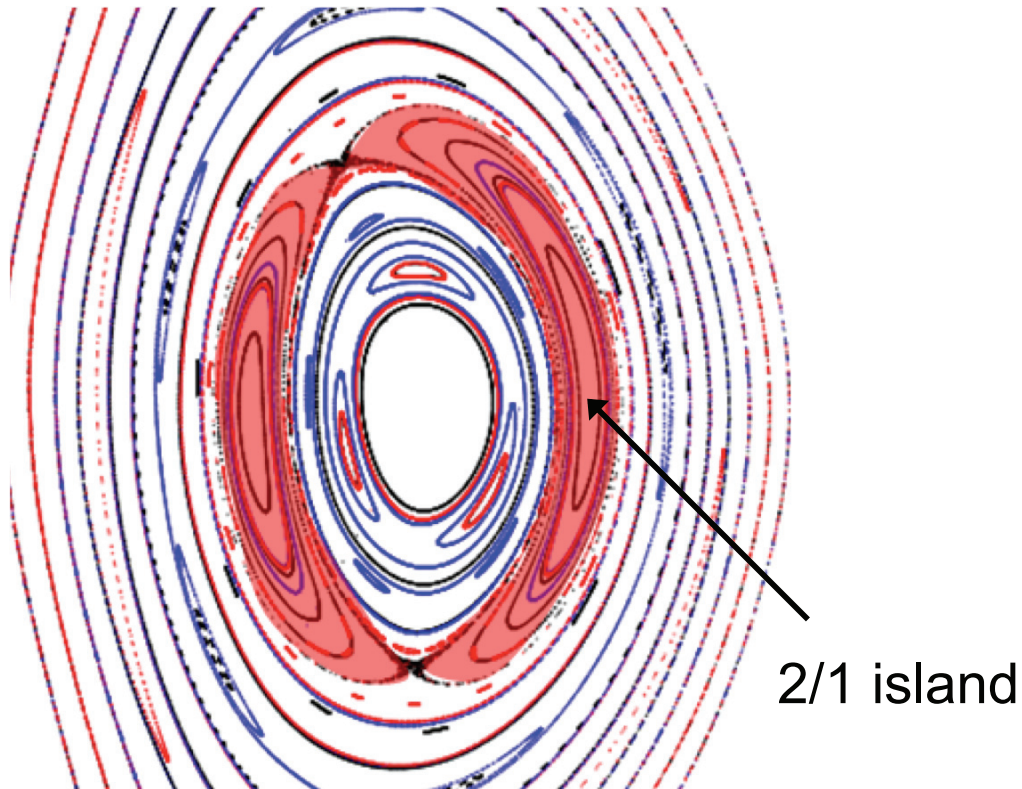
Analytic model reproduces features of the camera measurements



- Explains several features including location of X/O points
- Captures several line integrated effects:
 - Large on-axis perturbation
 - Deviation from flux surface off midplane

NIMROD simulates 2/1 island growth

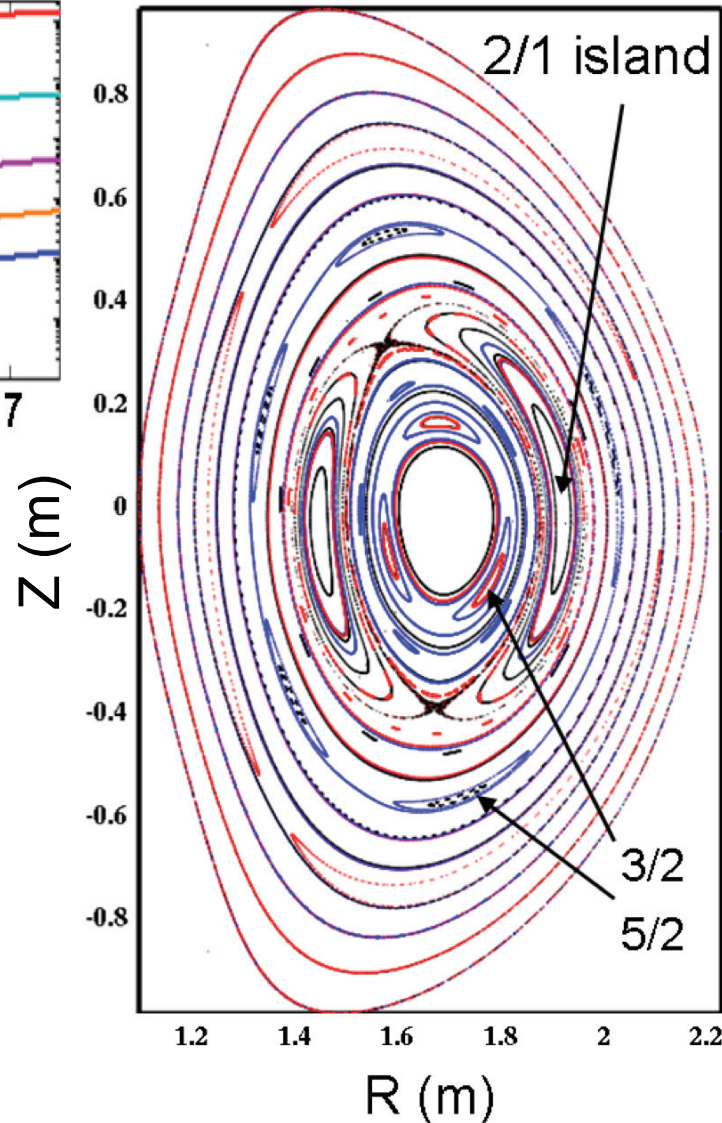
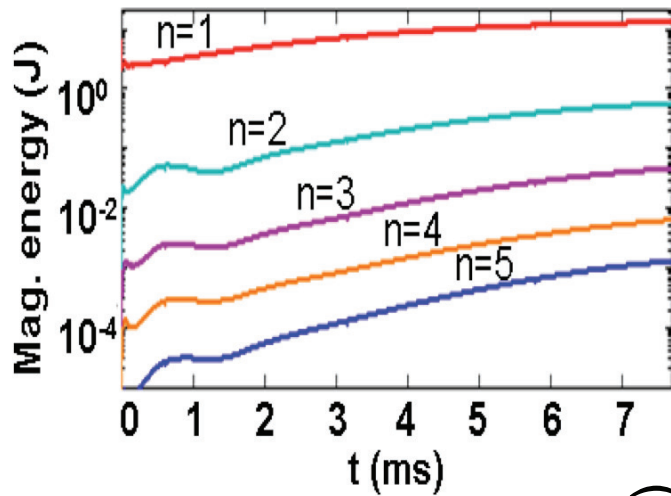
NIMROD is nonlinear, resistive, 3D MHD code.



Poincaré plot of magnetic field lines

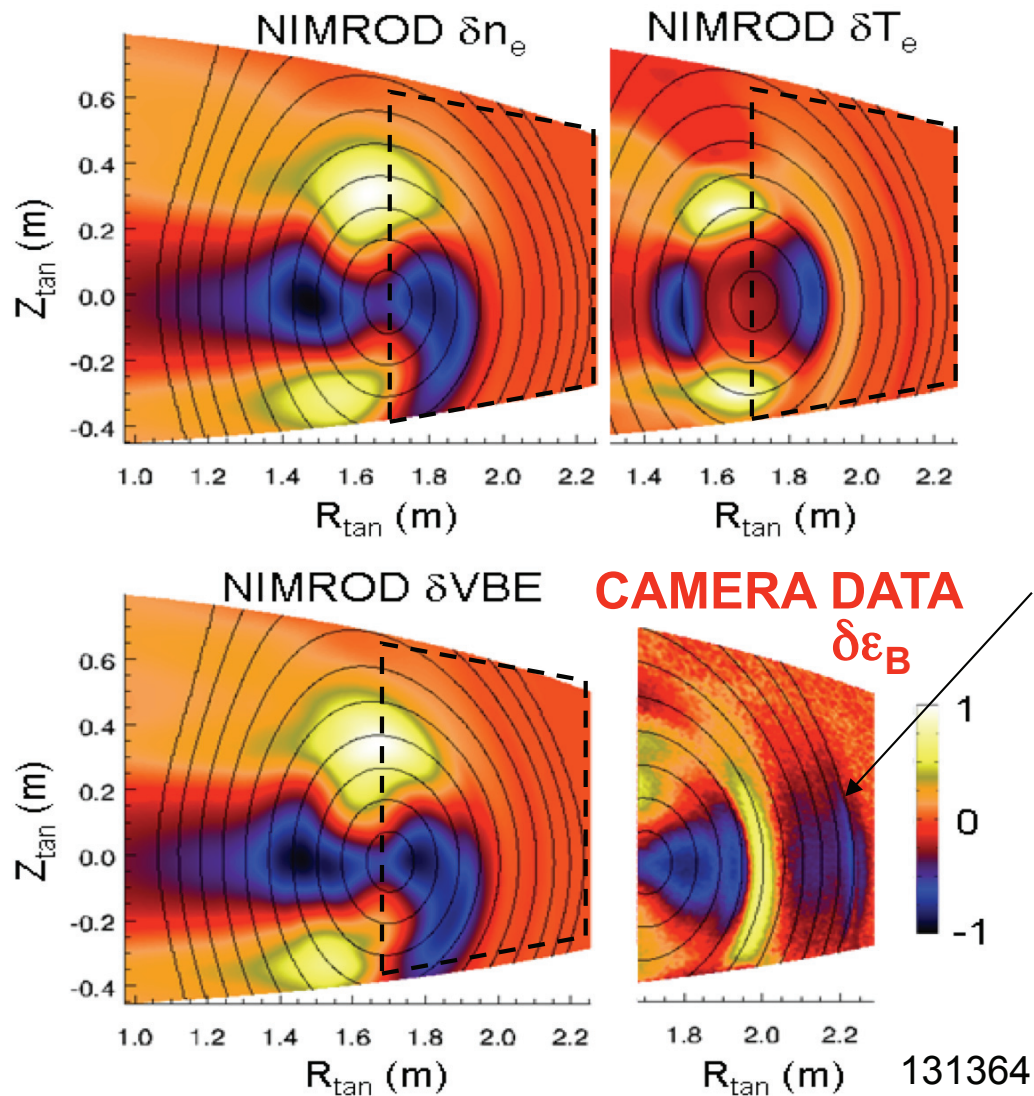
- Modeling begins with 2/1 seed island.
- Mode saturates at island width close to experimentally observed levels.

NIMROD simulates 2/1 island growth



- Modeling begins with 2/1 seed island.
- Mode saturates at island width close to experimentally observed levels.
- Other islands develop due to nonlinear interactions.

Synthetic camera diagnostic applied to NIMROD shows only marginal agreement with observations



All images are line-integrated

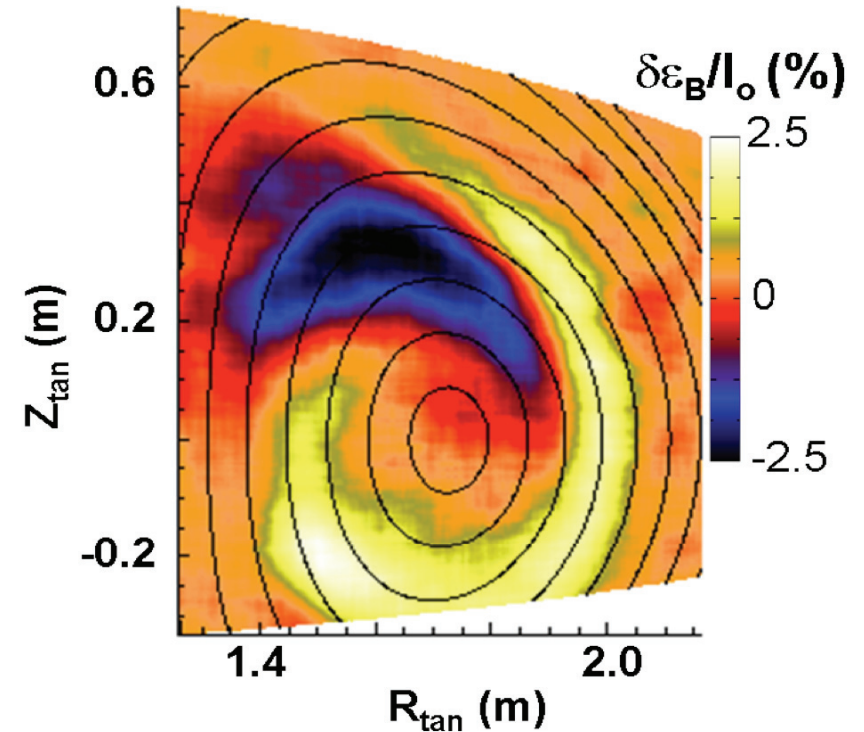
- High density diffusion of $10 \text{ m}^2/\text{s}$ used in code washes out island structures.
- Structure outside $\rho = 0.6$ in camera data may be due to surface deformation of plasma edge.

Outline

- Tearing modes.
- Sawtooth instability.
- Edge localized modes (ELMs).

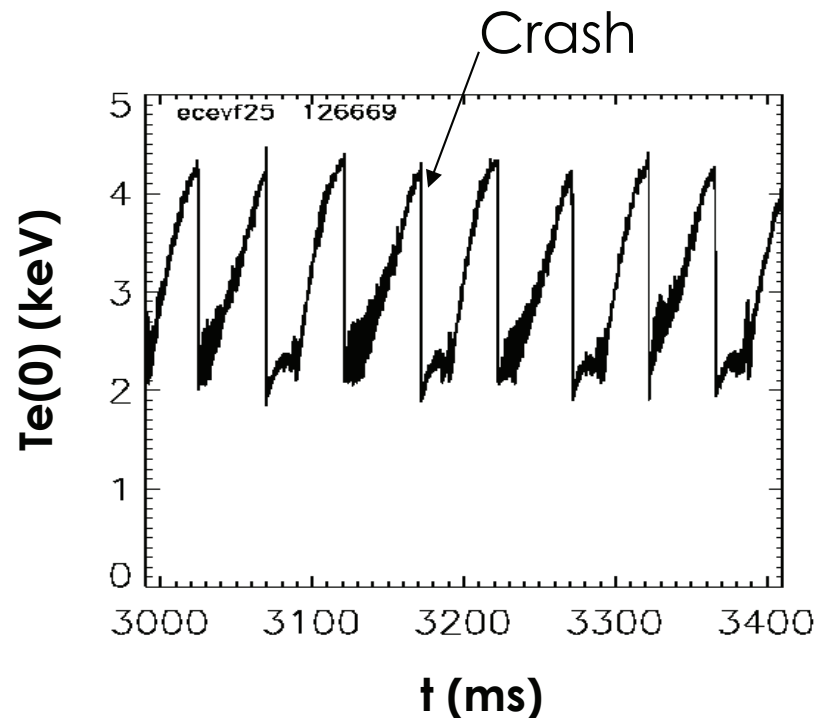
Previous sawtooth imaging:

- soft x-ray (Yamaguchi et al. 2004)
- ECE imaging (Park et al. 2006)



Sawtooth instability is a fast magnetic reconnection event

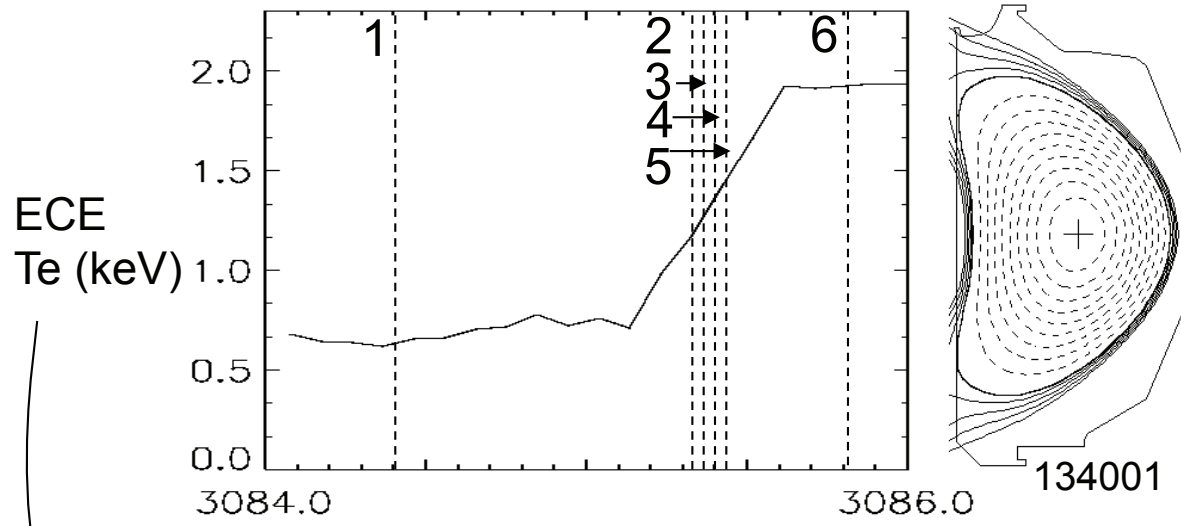
- Sawtooth crash is $m/n = 1/1$ explosive loss of heat and current in the core ($q < 1$) of tokamaks. Core temperature gradually builds up and cycle repeats.



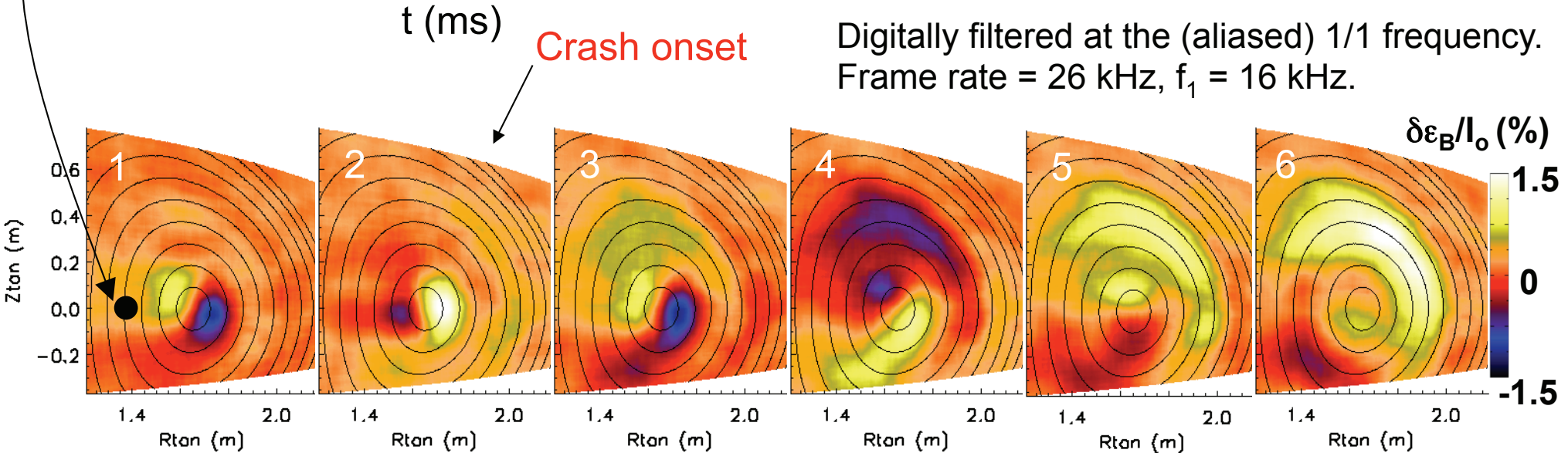
Sawtooth instability is a fast magnetic reconnection event

- Sawtooth crash is $m/n = 1/1$ explosive loss of heat and current in the core ($q < 1$) of tokamaks. Core temperature gradually builds up and cycle repeats.
- Outstanding issues:
 - Is magnetic reconnection partial or full?
 - Is sawtooth crash due to ballooning or kink modes?
- Imaging has potential to distinguish between sawtooth physics models.

Sawtooth crash creates VBE perturbation out to $\rho > 0.5$

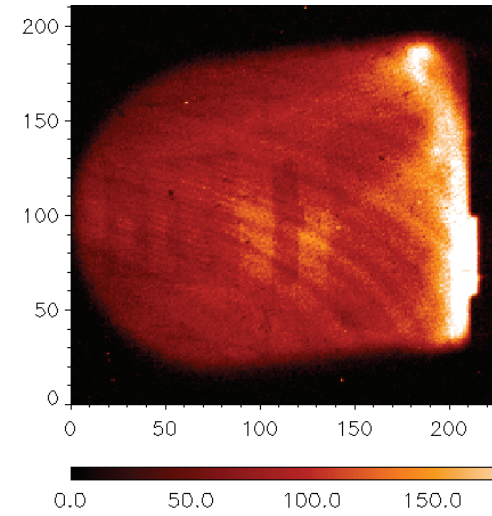


- $m=1$ precursor seen in bean shaped plasma.
- VBE pert. during crash appears poloidally localized.

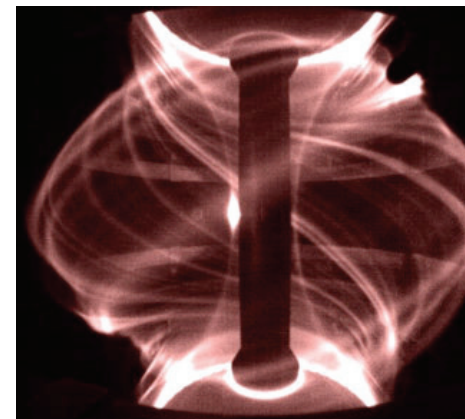


Outline

- Tearing modes.
- Sawtooth instability.
- Edge localized modes (ELMs).



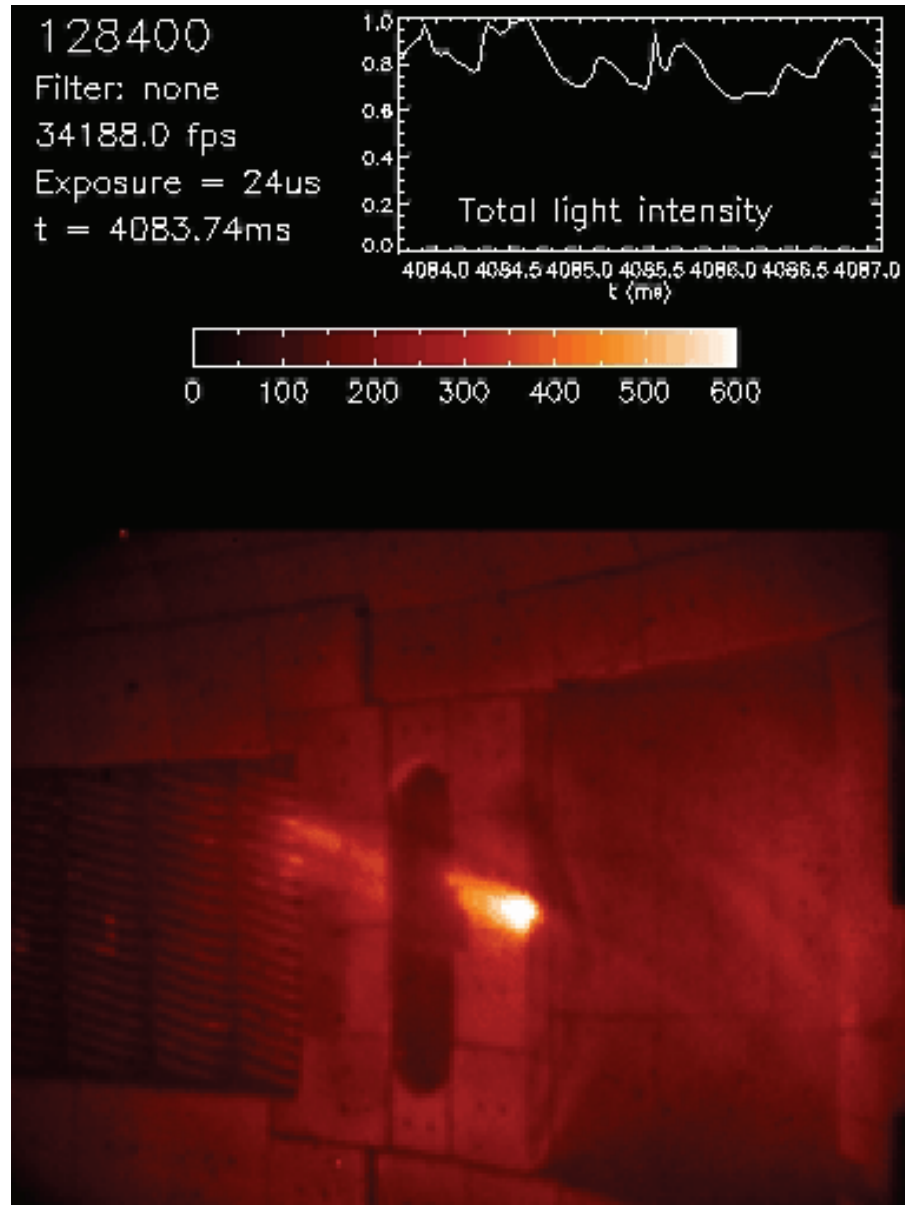
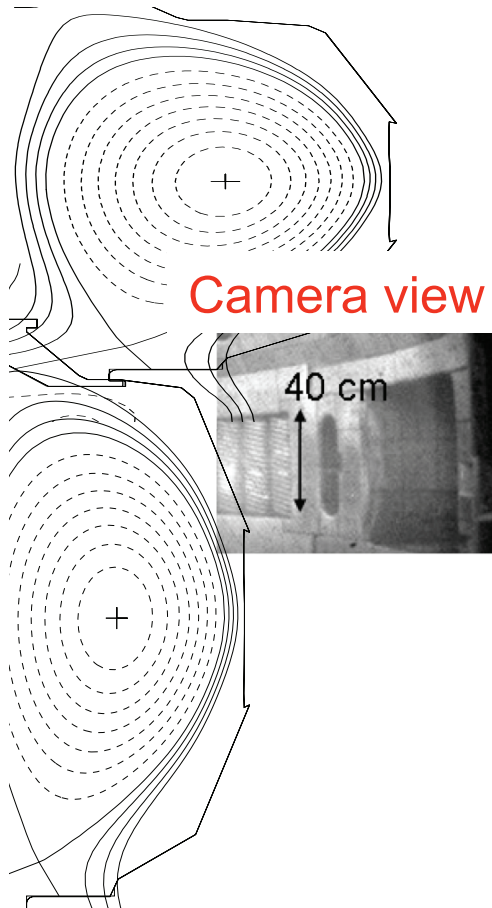
DIII-D



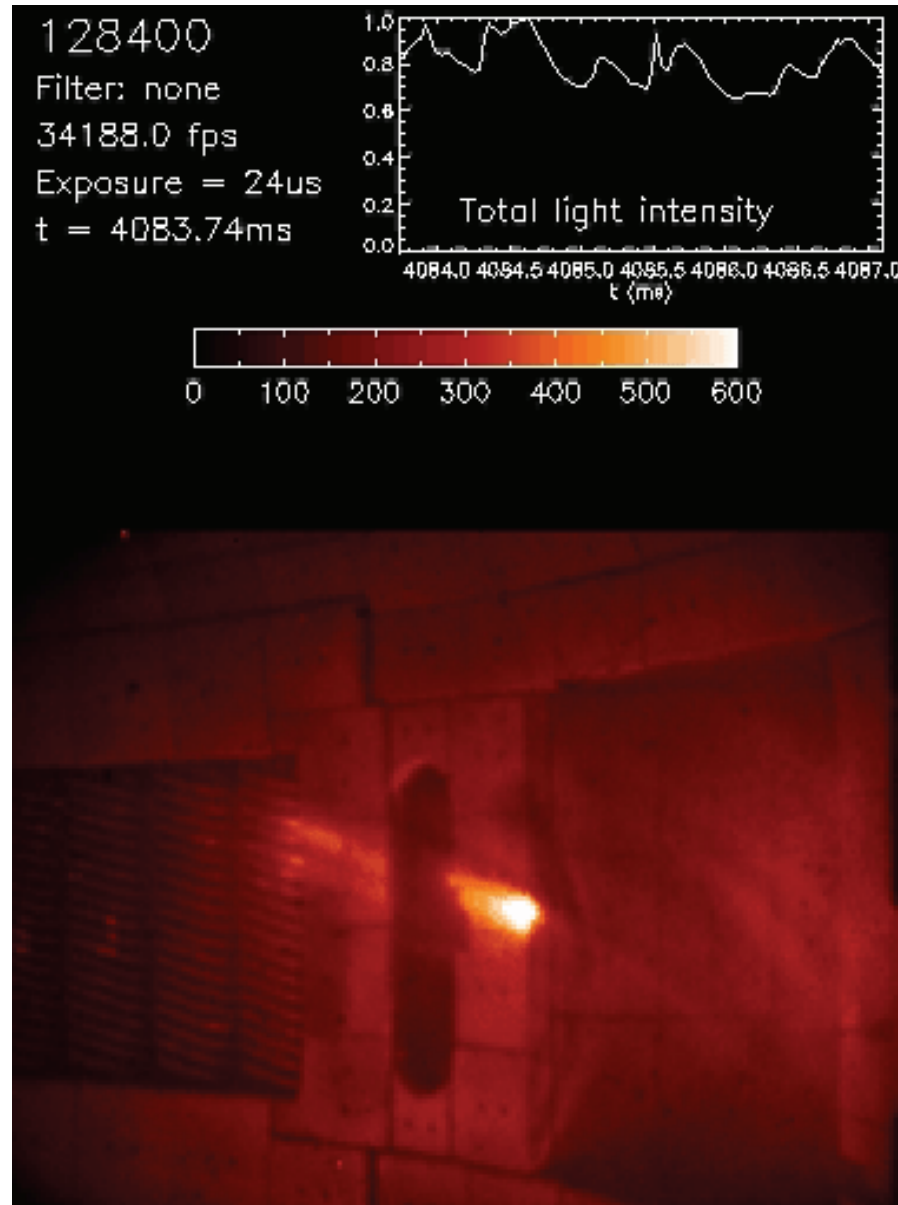
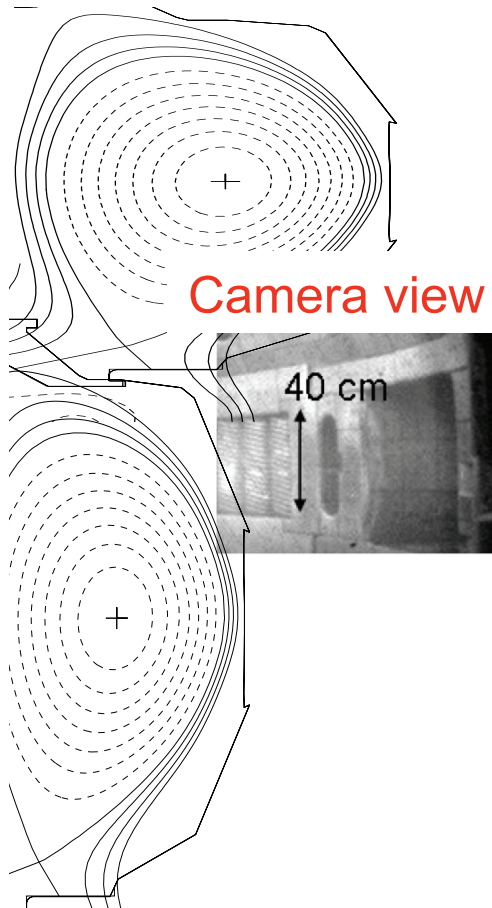
MAST

B. Koch, A. Herrmann,
A. Kirk et al., JNM 2007

During ELMs, multiple filaments interact with the outer wall

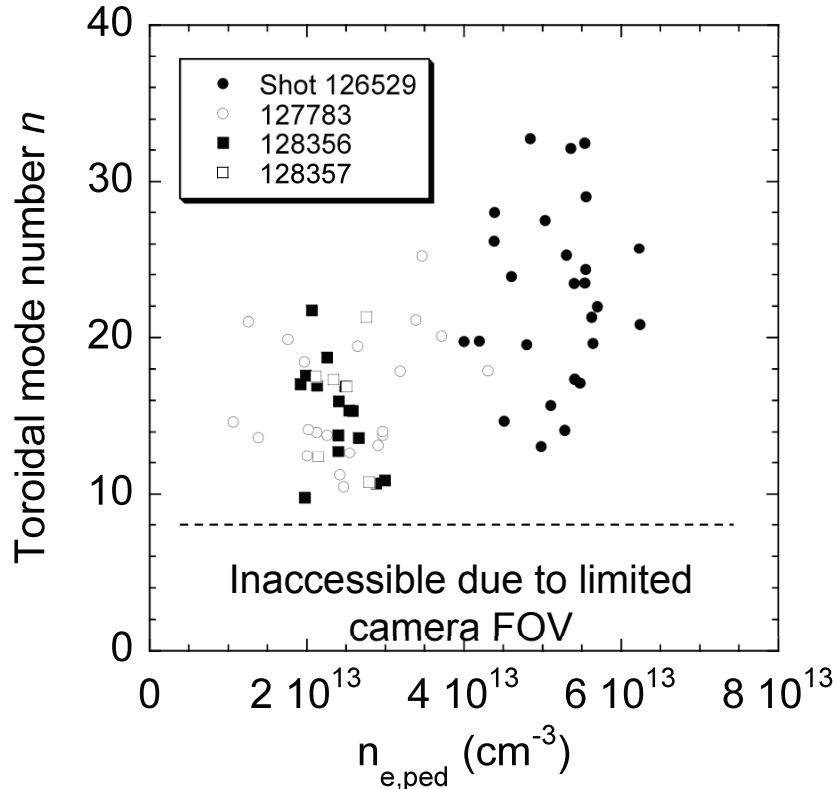


During ELMs, multiple filaments interact with the outer wall

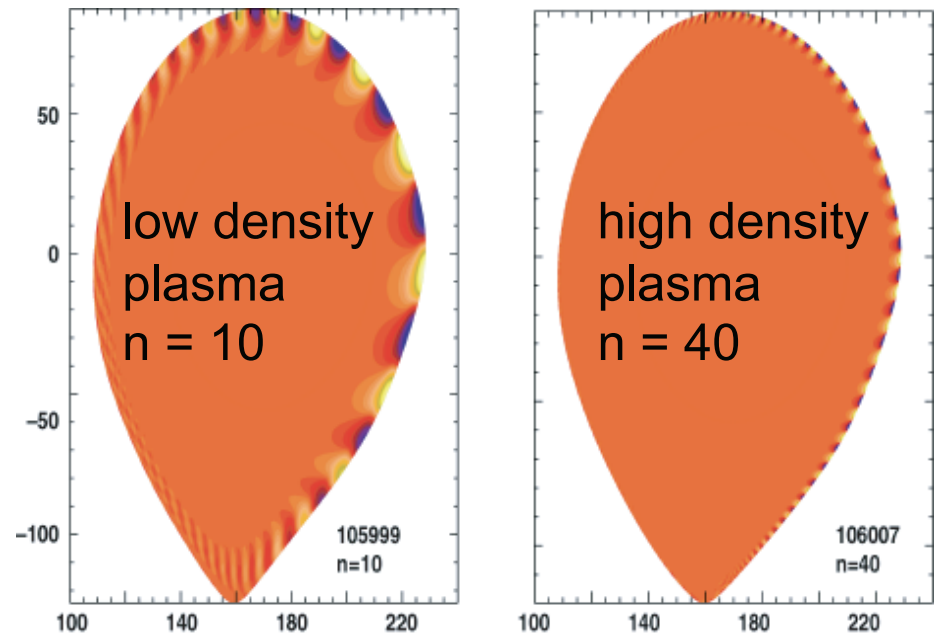


Measured ELM mode number is consistent with theoretical modeling

Mode number at onset of ELM.

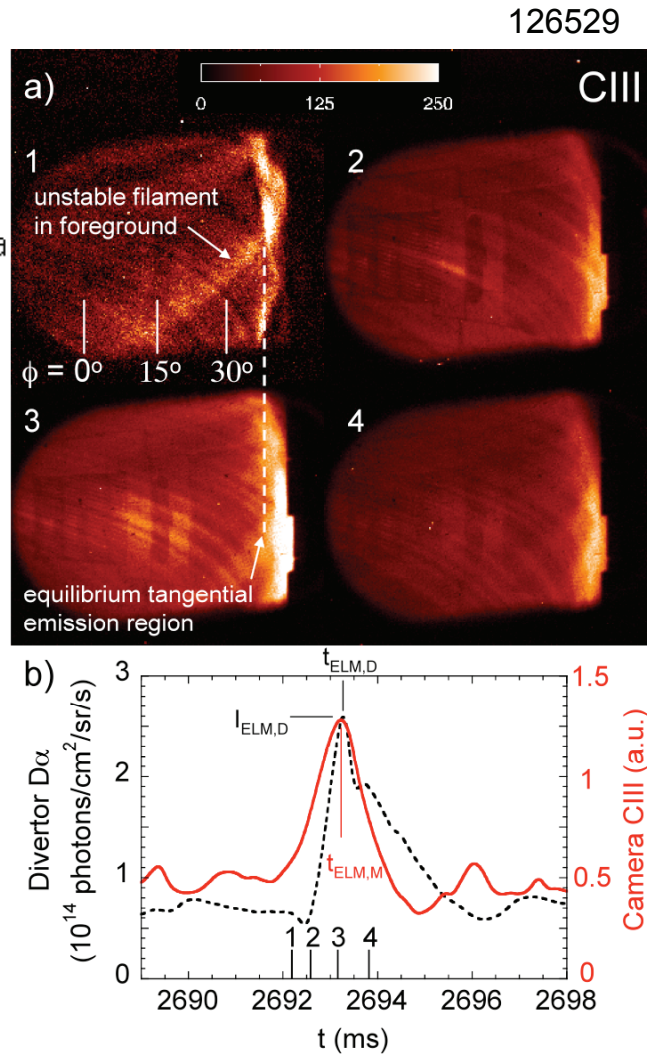
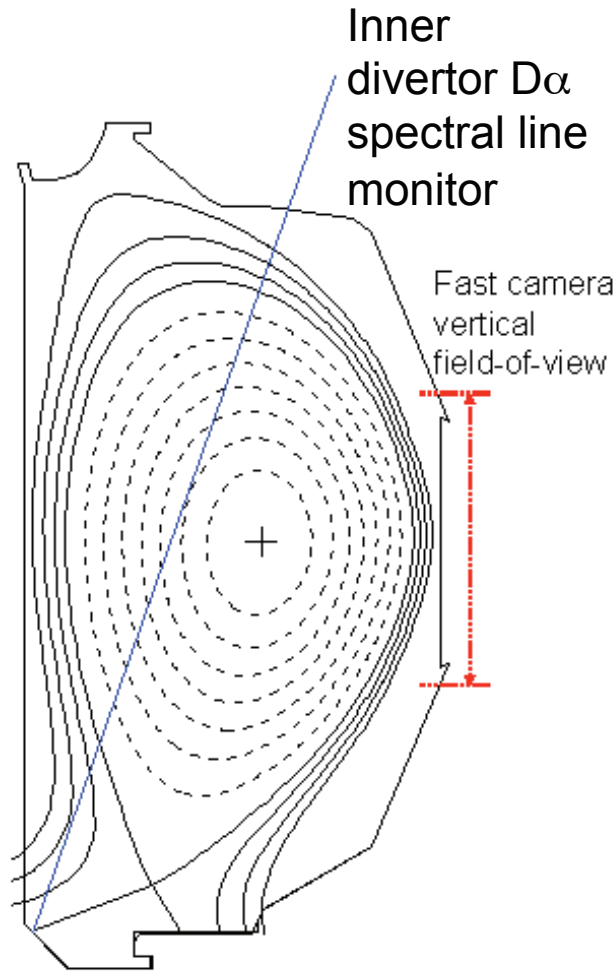


ELITE calculation of unstable mode structure just before an ELM

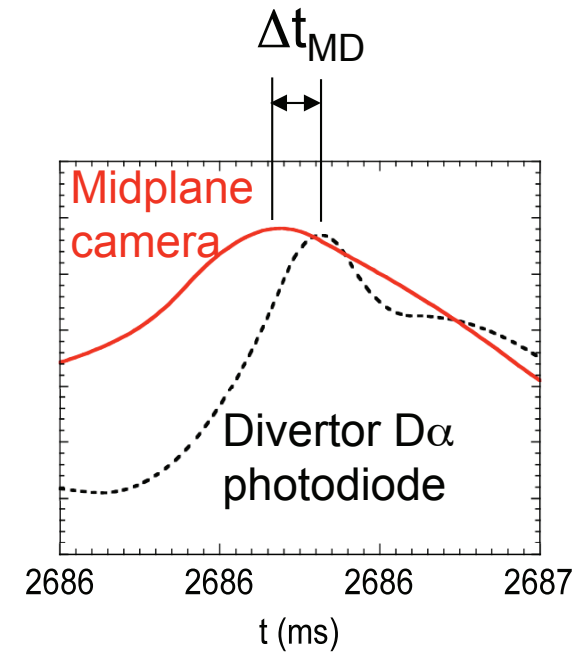


- Peeling \rightarrow current driven, low n . Ballooning \rightarrow pressure grad driven, high n .
- ELITE predicts higher mode number at higher density, due to collisional suppression of edge current.

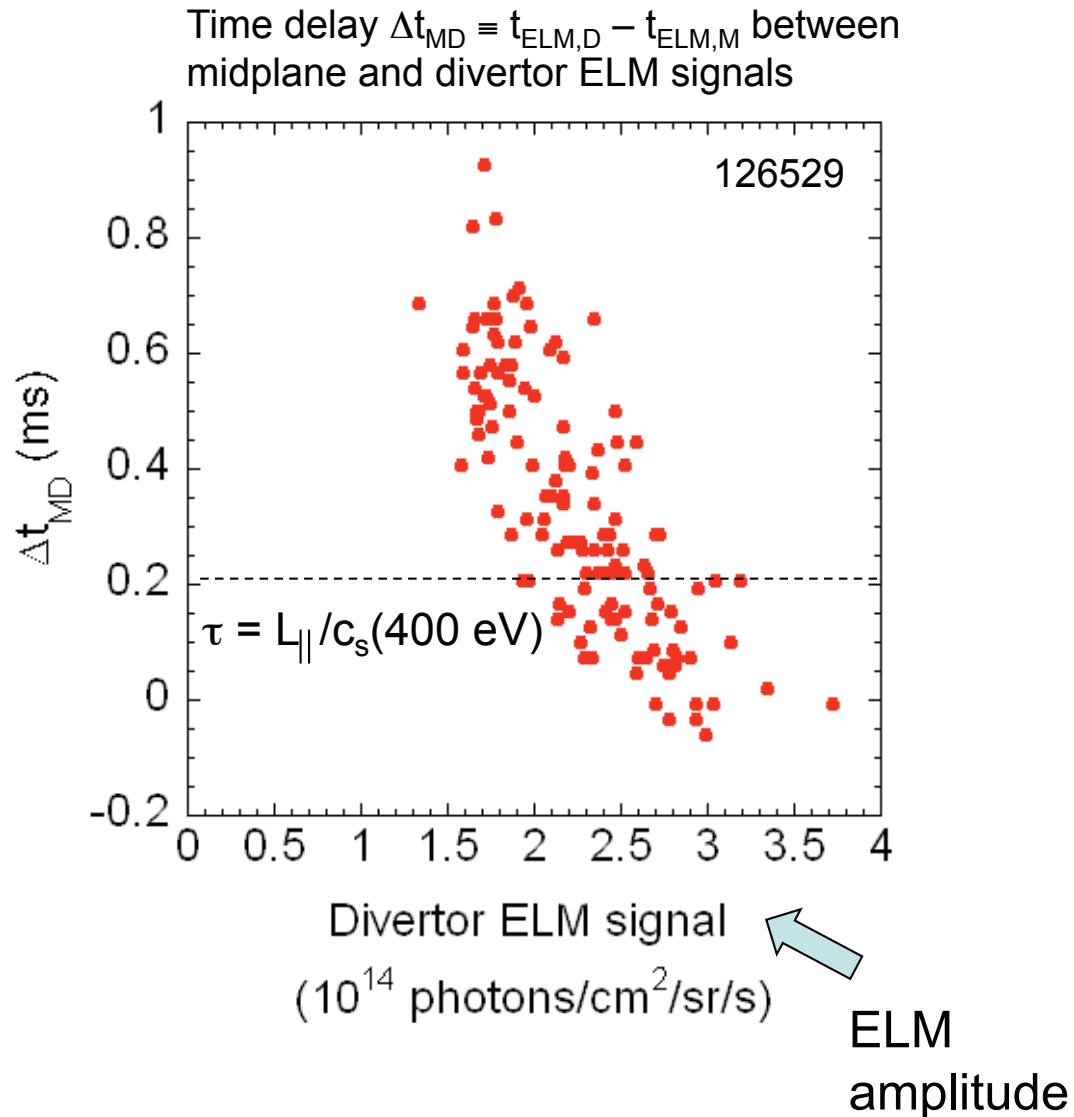
Parallel transport inferred from time delay between midplane and divertor ($D\alpha$)



Time delay Δt_{MD} between midplane and divertor ELM signals



ELM midplane-divertor time delay depends on ELM amplitude



Moderate collisionality $v_{ped}^* = 0.5$:

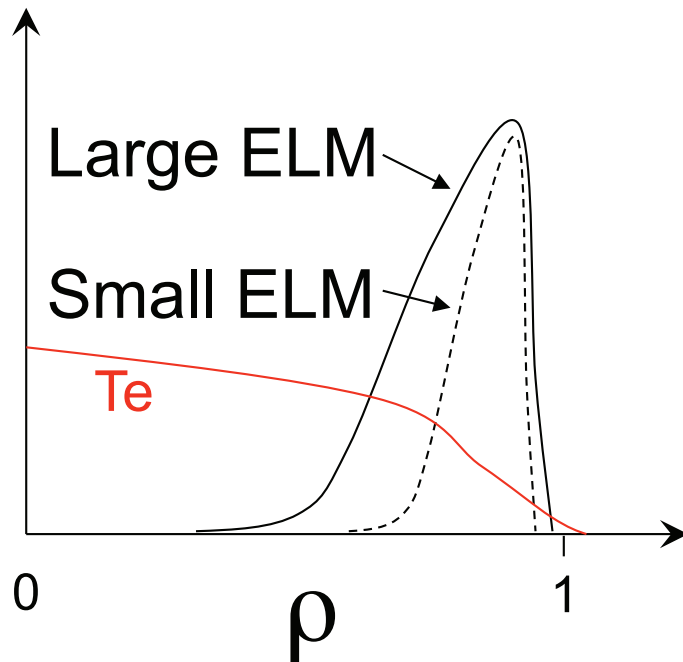
- ELM signal appears at midplane up to 800 μs **before** divertor.
- Parallel convective transport of ions in SOL¹.
- Ion parallel velocity depends on ELM amplitude.

¹Eich et al. 2003,
Fenstermacher et al. 2003,
Leonard et al. 2006,
Loarte et al. 2002.

Suggests ELM amplitude is related to eigenmode width

Osborne 2002

Eigenmode
amplitude, or $dP/d\rho$



Large amplitude ELMs have broader eigenmode structure



Hotter ions ejected into SOL from deeper within plasma



Faster parallel transport



Shorter midplane-divertor time delay for larger ELMs

Fast imaging allows detailed comparison to MHD models

- Direct imaging of structure and location of tearing mode islands may provide new tool for tearing mode control.
- Sawtooth crash with $m=1$ precursor creates poloidally localized VBE perturbation.
- ELMs have helical filamentary structure. Larger amplitude ELMs eject hotter ions originating further up the pedestal.